Atmospherically relevant chemistry and aerosol box model – ARCA box (version 1.2.~~0~~)

Petri Clusius[1*], Carlton Xavier[1*], Lukas Pichelstorfer[2], Putian Zhou[1], Tinja Olenius[3], Pontus Roldin[4], Michael Boy[1,5]

[1] Institute for Atmospheric and Earth Systems Research/Physics, University of Helsinki, P.O. Box 64, 00014 Helsinki, Finland
[2] Department of Chemistry and Physics of Materials, University of Salzburg, 5020, Salzburg, Austria
[3] Swedish Meteorological and Hydrological Institute (SMHI), SE-601 76 Norrköping, Sweden
[4] Division of Nuclear Physics, Department of Physics, Lund University, P. O. Box 118 SE-221 00 Lund, Sweden
[5] LUT School of Engineering Science, Lappeenranta-Lahti University of Technology, P.O.Box 20, 53851 Lappeenranta, Finland
* These authors contributed equally to this work.

Correspondence to: Petri Clusius (petri.clusius@helsinki.fi)

Abstract. We introduce the Atmospherically Relevant Chemistry and Aerosol box model ARCA box (v.1.2.~~0~~2). It is a zero-dimensional process model with focus in atmospheric chemistry and submicron aerosol processes, including cluster formation. Novel feature in the model is its comprehensive graphical user interface, allowing for detailed configuration and documentation of the simulation settings, flexible model input and output visualization. Additionally, the graphical interface contains tools for module customization and input data acquisition. These properties – customizability, ease of implementation and repeatability – make ARCA invaluable tool for any atmospheric scientist who needs a view on the complex atmospheric aerosol processes. ARCA is based on previous models (MALTE-BOX, ADiC and ADCHEM) but the code has been fully rewritten and reviewed. The gas phase chemistry module incorporates the Master Chemical Mechanism (MCMv3.3.1) and Peroxy Radical Autoxidation Mechanism (PRAM) but can use any compatible chemistry scheme. ARCA's aerosol module couples the ACDC (Atmospheric Cluster Dynamics Code) in its particle formation module, and the discrete particle size representation includes the fully stationary and fixed grid, moving average methods. ARCA calculates the gas-particle partitioning of low-volatility organic vapours for any number of compounds included in the chemistry, and the Brownian coagulation of the particles. The model has parametrisations for vapour and particle wall losses but accepts user supplied time and size-resolved input. ARCA is written in Fortran and Python (user interface and supplementary tools), can be installed on any of the three major operating systems and is licensed under GPLv3.

Introduction

Aerosol and chemical models can be categorized by their dimensionality, where zero-dimensional models are called box models. However, a box model is generally used as a core module in dimensional models (column, regional or global models), and therefore it makes sense to further describe a model by its complexity and level of details in the chemistry and physics. In this respect, aerosol models can be divided in sectional or modal approach, where the first uses discretized size representation and the latter treats the aerosol population as a combination of modes (Zhang et al. 1999). The modal approach is often used in global models due to computational efficiency (e.g. the M7, Vignati et al. 2004), but as the sectional approach can be kept coarse enough, models such as SALSA (Kokkola et al. 2018) have found their place in large scale use as well as smog chambers. Here we turn our focus to sectional models with detailed chemistry and aerosol processes, which find ~~wide~~their use in ~~many practical air quality~~smog chamber, flow tube or ~~environmental questions~~atmospheric conditions. During the last decades of atmospheric research, several numerical process models for simulating gas and particle phase chemistry and dynamics have been developed. Examples from recent years include (but are not limited to) KinSim, used in simulating the chemical evolution of various gas phase species aimed at studying indoor-air chemistry (Peng and Jimenez, 2019), or MAFOR (Multicomponent Aerosol FORmation model, Karl et al. 2022), also a community aerosol dynamics model which includes

multiphase chemistry. Often models are focusing on some particular aspect of aerosol dynamics, such as nanoparticle chemistry and dynamics, e.g. MABNAG, (Yli-Juuti et al. 2013) and TOMAS and its extension SOM-TOMAS (e.g. Adams and Seinfeld 2002; Akherati et al. 2020), particle chemistry and fine structure (e.g. KM-SUB, Shiraiwa et al. 2010) or cloud

45 droplet chemistry and processes (CLEPS, Rose et al. 2018). A review paper by Smith et al. (2021) discusses the current status of the understanding of nanoscale aerosol chemistry, and also gives a good overview of the many process models that are used to solve aerosol and atmospheric chemistry and dynamics.

The history of ARCA box starts from the four models used by the authors: MALTE-box (Boy et al. 2006; Boy et al. 2011), ADCHEM (Roldin et al. 2011; Roldin et al. ~~and~~2014), ADiC (Pichelstorfer and Hofmann 2015) and ACDC (Atmospheric

50 Cluster Dynamics Code, McGrath et al. 2012; Ortega et al. 2012). These models have been used to study ambient phenomena ~~(e.g., Boy et al.~~, test and ~~2006; Boy et al. 2011; Roldin et al. 2011; Roldin et al. 2014; Roldin et al. 2019),~~ study complex chemical schemes ~~(e.g., Boy et al. 2013; Xavier et al. 2019) or~~ or specialized applications such as molecular clustering, chemistry and deposition in lungs (e.g., ~~Pichelstorfer and Hofmann 2015~~Olenius et al. 2013; Myllys et al. 2019; Boy et al. 2013; Pichelstorfer ~~et al. 2021).~~and Hofmann 2015; Xavier et al. 2019; Pichelstorfer et al. 2021). The current work is the

55 amalgamation of these models, with the aim of further development as an open-source community model.

When a scientist without prior experience of a detailed process model wants to apply ~~one~~a detailed aerosol process model, often practical problems arise. Many of the models require substantial modification of source codes and programming experience to be applicable for a given case study. Available models are usually tailor-made for a particular problem and might not be written with flexible enough code (for example, parameters are hard-coded) and consequently be vary laborious to set

60 up. Setting up a model involves detailed configuration, usually requiring in-depth knowledge of the code structure, and contains high risk of misconfiguration. The more the model code needs to be modified, the more the probability of introducing bugs increases. These are some reasons why applying complex numerical models can be unappealing. For most scientists, the simulation itself is not the main focus or motivation of the work, and one would prefer flexible and easily applicable tools, with minimal risk of misconfiguration, and with reasonable amount of time spent in familiarization with the tool. Recently,

65 Python-based solutions have become available, e.g., PyCham (O'Meara et al. 2020) and PyBox (Topping et al. 2018). Yet, it can be said that in terms of usability, the scientific tools are not on par with current-generation software in general. To meet these challenges, we introduce the 0-dimensional Atmospherically Relevant Chemistry and Aerosol box model ARCA box ~~v1~~ (v.1.2.~~0~~2). One of the objectives of the development has been in applicability of the model. It is flexible regarding the complexity of the chosen chemistry and aerosol composition as well as the timescale of the simulation. The backbone of ARCA

70 consists of established theories and standard model implementations, but the model is flexible to customization and further extensions. The source code is written in a way that enables the use of additional or substituting parametrizations for the modelled processes. However, the major advantage of ARCA, setting it apart from other current models in its field, is the graphical user interface (referred from here on as GUI). It makes the model easier to apply, greatly increases reproducibility, reliability and documentation of the simulations, provides tools for visualisation of the output and automatizes many steps in

75 model setup and configuration.

This paper is structured in the following way: Section 1 introduces the scope of the model and explains its structure and main functionality. Section 2 describes the scientific theories behind the modules. Section 3 explains the usage of the model, focusing on the graphical user interface. Section 4 shows verification and standard evaluation of the model's modules. Section 5 summarises technical details about the system requirements, installation, licensing, code availability and further documentation

80 (the ARCA online manual). Section 6 concludes this paper with plans for future development.

When text is written in MONOTYPE, it refers to a user-definable variable name, which are available from the GUI. Full list of these input variables is shown in Appendix A.

1 Scope and uses of the ARCA box

ARCA box is primarily intended to be used for studying processes such as gas phase chemistry and aerosol processes at atmospherically relevant concentrations (trace gases) and conditions (pressure, temperature, humidity, irradiance). A box model is typically used for simulating smog chambers, indoor spaces or other small containers. Additionally, it can be used to simulate ambient (field) processes, as long as the assumption of homogeneity of the conditions are met (see 1.1). Using a box model instead a dimensional model in outdoor simulations is beneficial because computational resources can be put in more detailed chemistry and aerosol processes. ARCA is therefore well suited for studying complex processes and developing and testing new (chemical, aerosol, etc.) schemes, before implementing them in a dimensional model. In addition to scientific research, due to its ease of use and configuration ARCA has also been used in teaching of aerosol chemistry and physics.

Given a proper chemistry scheme the model can be used to study formation of chemical compounds from precursors (or their emissions), calculate effective reactivities (inverse of chemical lifetime) with chosen reactants, and simulate the effects of dynamically varying conditions to these processes. The particle formation rate module, containing the Atmospheric Cluster Dynamics Code (ACDC, McGrath et al. 2012; Ortega et al. 2012) simulates the production of new nanoparticles by clustering of molecules – by default from H_2SO_4–NH_3 and H_2SO_4–Dimethylamine (DMA) mixtures, but any chemistry can be included, given compatible input data. Any organic compound in the chemistry scheme, whose pure liquid saturation vapour pressure is known (or estimated), can contribute to particle growth by condensation as calculated by the Analytical Prediction of Condensation (APC) scheme (Jacobson 2005). Aerosol processes further include coagulation losses and growth by Brownian coagulation, and losses by external sink such as wall losses. Because any of these processes can be switched on or off, quantifying their effects to the total dynamics is straightforward. The GUI allows model initialization and constriction in different ways, ~~using~~ either through predefined values from files (such as measurements), or by parametric, time dependent functions, configured graphically in the GUI. Sensitivity studies, used to assess the effects of uncertainties and variability of the model parameters, are done by changing the parameters within some range. To this end, the GUI has tools to create batches of simulations, where the nominal time dependent input parameters for selected variables are varied (either by multiplying or shifting) within user defined ranges and intervals.

1.1 Main assumptions of the model

Like any box model, ARCA does not consider spatial variation and the related processes, most importantly advection (including convection). When simulating ambient (field) processes, we must therefore assume that the conditions are spatially homogeneous. The transport equation, describing the local change of scalar variable S in terms of its total derivative and advection in wind field $\vec{V}$, then becomes

$$\frac{\partial S}{\partial t} = \frac{dS}{dt} - \vec{V}\nabla S \approx \frac{dS}{dt} \tag{1}$$

which is acceptable approximation when $\left|\frac{dS}{dt}\right| \gg |\vec{V}\nabla S|$, as is the case with fast chemical reactions, but not necessarily for slow processes like aerosol growth and coagulation losses. This alone will produce inevitable deviation between modelled (following dS/dt) and locally measured (following $\partial S/\partial t$) time series.

~~In~~The particles in the discrete aerosol ~~module particles~~size distribution are assumed to be spherical, liquid-phase droplets with constant density (ORGANIC_DENSITY). Charges are omitted and all particles ~~in the aerosol module~~ are treated as electrically neutral (ion-mediated nucleation is ~~simulated~~considered in ACDC module, which calculated the stable cluster formation rate). Liquid phase organic chemistry in the particles, for example polymerization and the consequential effects this has on the thermodynamics (sometimes called ageing) is not considered in the model. In the present model version particles of all sizes – even above activation diameter – are completely void of water and the dissolution of inorganic compounds is therefore ignored. Some of these restrictions will be addressed in the near future updates ~~(see section 6).~~; see Sect. 6, which also discusses some of the possible implications of the currently missing particle phase chemistry.

The ACDC nucleation module is more flexible than the aerosol module and – given the proper input – would be capable of simulating also hydrated clusters, but presently neither of the included cluster chemistry systems contain hydrated clusters.

1.2 Structure of the model

The main processes modelled in ARCA box are (in the order of execution): 1) gas phase chemistry 2) formation of molecular clusters 3) reversible vapour wall ~~loss~~losses 4) gas-particle partitioning (condensation and evaporation, using the APC scheme) 5) coagulation of particles 6) wall loss of particles (Fig. 1). The processes – which can be switched on and off in any combination – are executed in a series where the next process relies upon values which were calculated in the previous process.

Compared to a method where all changes within time step are solved as one coupled system, this has the advantage that adding more processes (or skipping them) is straightforward as they can simply be added to the main loop as a subroutine or module and solved in any suitable way. On the other hand, the forward integration requires that the time step is kept small enough to justify the linearisation of a non-linear system. The default time step (10 seconds) is usually a good compromise between stability and computational efficiency, but the model also includes a time step optimization algorithm (described in Sect. 1.3).

Programmatically the model consists of two main parts: the numerical model (in Fortran), which should be compiled on the computer where it is executed, and the graphical user interface GUI (in Python). Both software environments are freely available in Windows, Mac and Linux, and the model has been successfully installed and used on all three platforms. The numerical module is configured and initialized with a setting file, called hereafter as INITFILE, defining all the simulation settings. Additional input includes the spectral irradiance or actinic flux, pure liquid saturation vapour pressures of low-volatility organic compounds and (optionally) the elemental composition of the condensing vapours, and (also optionally) time series of environmental variables, precursor gases, initial or background aerosols and aerosol loss rates, if the built-in parametrization is not used.
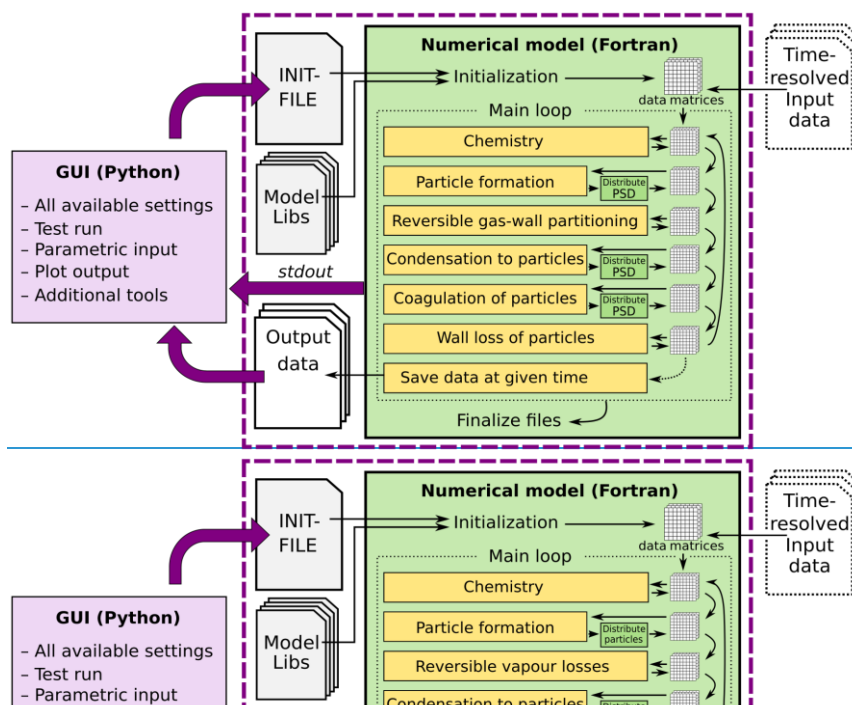
1.3 Model time step optimization

The model can be used with a fixed time step DT (default time step is 10 s) or with multiple, dynamically changing time steps. With latter the user defines the maximum and minimum relative change in one time step for 1) particle diameter (dd_p), 2) particle number concentration in each bin (dN_p) and 3) concentration of condensable vapours (dC). After exiting each module (shown in Fig. 1), the changes in 1–3 are calculated. If the module produced changes that exceed the maximum, the time step

for that module is halved and the current integration time step will start over. In contrast, when the largest change is below the
150 tolerance minimum, the time step of that module is doubled. The modules are assigned with one of the three time steps, denoted
CCH (condensation and chemistry), COA (coagulation) and DEP (losses). The processes used to control the time steps are
shown in Table 1.

Table 1: Time step optimization.

Module	Time step	Defining process
Chemistry	CCH	dC; if the Condensation module is used, chemistry does not affect time step; otherwise, dC is calculated for compounds whose concentration is above `MIN_CONCTOT_CC_FOR_DVAP` (default 1000 molec/cm³)
Particle formation	min(1,2,3)	[does not affect time step]. When used without other modules, time step optimization is not available.
Chemical wall loss	CCH	[does not affect time step]
Condensation	CCH	dC, dD_p; dC is calculated for compounds whose concentration is above `MIN_CONCTOT_CC_FOR_DVAP`
Coagulation	COA	dN_p
Particle losses	DEP	dN_p

155 When time step optimization is used, a 3-element vector `DT_UPPER_LIMIT` defines the maxima for CCH, COA, and DEP, and
the nominal model time is used as a minimum (by default the GUI sets `DT` to 1 ms). Therefore, the three time steps are defined
by multiplying the nominal model time step by a factor of 2^n, where n = {1, 2, 3…}, and satisfy `DT`$<\Delta t \times 2^n \leq$ `DT_UPPER_LIMIT`.
Optimizing time step this way has two effects. It helps to overcome the potential error created by decoupling of different
modules that are not solved together as one dynamic equation (notably condensation to particles and chemistry) by
160 guaranteeing that the changes in one time step are small. On the other hand, when a process is very slow, such as aerosol
coagulation, the extra precision gained by small time step is negligible; instead increasing the time step can shorten the
computational time significantly. The effect on the execution time of the simulation depends on the tolerances and the
conditions of the simulation. With loose tolerances (5–10%) the simulation time is usually shortened, while tight tolerances
(0.2–3%) will increase runtime markedly. The time step optimization should first and foremost be seen as a safeguard against
165 diverging too far from the true solution of the integration.

2 Modules of ARCA box and their theoretical base

2.1 The chemistry module

The chemistry code of ARCA is based on the KPP (Kinetic PreProcessor, https://people.cs.vt.edu/asandu/Software/Kpp;
Damian et al. 2002), and any reaction set which complies with the KPP format can be used to create ARCA's chemistry
170 modules. An often-used source for atmospheric chemistry scheme is the MCM v3.3.1 (Master Chemical Mechanism version
3.3.1, http://mcm.leeds.ac.uk/MCMv3.3.1) (Jenkin et al. 1997; Saunders et al. 2003; Jenkin et al. 2015), which provides the
gas-phase chemical reactions and rates of the degradation of specific organic compounds in the atmosphere, as well as detailed
inorganic chemistry and photochemistry. The full scheme – or a subset – can be downloaded from MCM website in KPP
format. Optionally, the user might have additional chemistry schemes, which need to be combined with the MCM scheme,
175 such as the PRAM scheme (Peroxy Radical Autoxidation Mechanism; Roldin et al. 2019) which describes the production of
highly oxygenated molecules (HOMs) from monoterpenes and is included in the ARCA distribution. ARCA's GUI has a tool
("Create chemistry scheme") which combines different schemes, removes duplicate compounds and reactions and creates a
valid single KPP definition file, used for producing a Fortran module with KPP. A modified source code of KPP v2.2.3,
accommodated for very large schemes, is provided with ARCA. The generated code will then be part of ARCA and is available

180 for use after compilation. Switching between different chemistry schemes can later be done in the GUI with a ~~dropdown~~drop-down menu.

2.1.1 Photochemistry

The photolysis rates of the photochemical reactions are calculated by integrating the absorption cross section, quantum yield (provided by MCM v3.3.1), and actinic flux (AF). Actinic flux spectral data (in ~~W m⁻²~~photons cm⁻² s⁻¹ nm⁻¹) can be sent

185 directly in or it can be estimated from the global short-wave radiation (~~also~~ in W m⁻² nm⁻¹), surface albedo, geographic location and the date of the simulation, as described in Kylling et al. (2003). The actinic flux and short-wave radiation are wavelength dependent, but often only the total irradiance over a wavelength range is measured, instead of the spectral distribution. ARCA contains a generic clear sky spectrum (*glob_swr_distr.txt*) between 280 nm – 4.8 μm, obtained from the Bird Simple Spectral Model (Bird and Riordan 1986). There is also a site-specific spectrum for SMEAR II station in Hyytiälä, Finland, based on

190 measured and averaged yearly spectra from 2001 (Boy and Kulmala 2002). The spectrum in *glob_swr_distr.txt* is normalized for 300 nm – 4 μm wavelength range, assuming a flat response from the instrument. Should the actual measurement range differ from this, the user can provide the lower and upper limits of the wavelengths, and the default spectrum will be normalized to this range.

The provided two spectra are somewhat generic and represent field conditions. For more precision – or e.g., smog chamber

195 simulations – the user should provide their own spectral data which must be in 5 nm steps and contain entries from 280 nm to 700 nm. Exceeding entries in the data file are ignored as they are not relevant in the photochemistry. Spectral data can be a single, constant spectrum or time-resolved. If time dependent data is provided, a linear interpolation in time is performed at each model time step. The exact format of the spectral file is described in the online manual.

The user supplied spectral data can either be thought as a weighing function, whose integral over the measured wavelength

200 range amounts to 1, or as absolute values [W m⁻² nm⁻¹]. In the first case the time-dependent scalar variable SW_RADIATION represents the measured total irradiance, and in the latter SW_RADIATION is set to a constant (1, or some dimensional factor). Finally, if the option SWR_IS_ACTINICFLUX is selected, the SW_RADIATION and the provided spectral data is directly used as actinic flux. [photons cm⁻² s⁻¹]. A schematic representation of the short-wave radiation data processing is shown in Fig. 2.
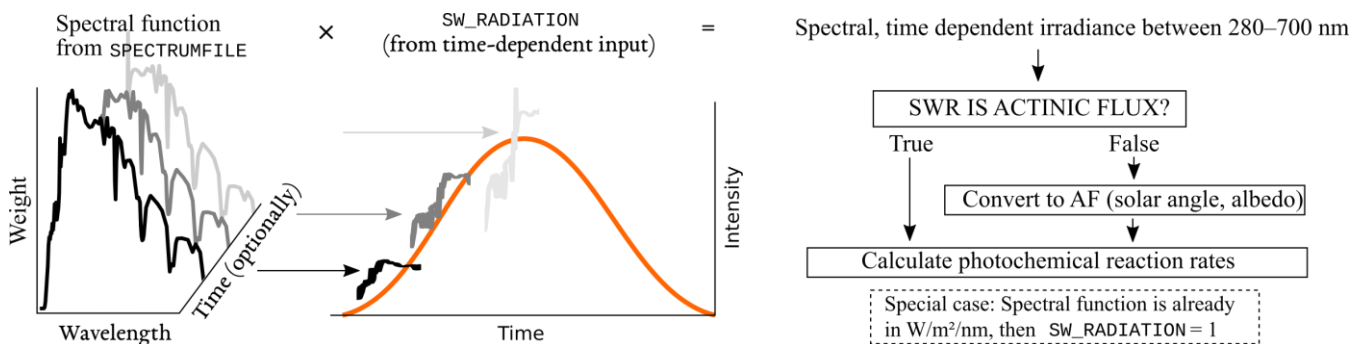
Figure 2: Schematic representation of how actinic flux is calculated from the provided input.

205 ### 2.1.2 Reaction kinetics

At each time step, the reaction rates (including photolysis) are updated using current pressure, humidity, irradiation and temperature. With these the chemistry module solves the new concentrations after one model time step. The concentration C of any compound q is described by the ODE

$$\frac{dC_q}{dt} = \sum_{x=1}^{N_q} R_{x,q} \tag{2}$$

where $R_{x,q}$ are the reactions x that either produce or consume the compound q. The ODEs of the compounds in the chemistry

210 scheme form a system of coupled non-linear equations, which is solved numerically in ARCAs chemistry scheme, by default using KPPs general Rosenbrock solver (Sandu et al. 1997).

In ARCA the concentration of any compound in the chemistry can be set to a user defined value. Typically, this is done for the precursor gases, whose concentrations could be measured or otherwise known. The user supplied concentrations are read from the input, interpolated to model time and saved in the model data matrix, overwriting previous values. Then, if a

215 compound was defined as fixed in the chemistry scheme (DEFFIX in KPP definition file), its time derivative (eq. 2) is zero, and the concentrations do not change during the chemistry step; if the compound was not fixed (DEFVAR in KPP definition), the concentrations will in general change (and this would be reflected in the concentrations of its reaction products), but as previously, the resulting concentration will be overwritten in the next time step when the model concentration is set to the given input concentration. The user can also define a time after which the updating of the concentrations of the chemical

220 compounds (and separately for emissions) is stopped, and the chemistry is let to "float", meaning that also the precursor concentrations evolve dynamically without outside interference (if they are DEFVAR). The definition of fixed and varying compounds can easily be done in ARCAs "Create chemistry scheme" tool when creating a new chemistry scheme. As a rule, precursors should be defined as fixed, unless the simulation involves floating of the chemistry, as described above. Figure **Error! Reference source not found.** further explains the effect of these settings to the simulation.

225 After the chemistry step, all negative values are set to zero. Negative concentrations are non-physical but could emerge from numerical inaccuracies, so a warning is issued if some concentration is less than –100 molec/cm³, as this would be an indication of misconfiguration, such as wrong units in the input.
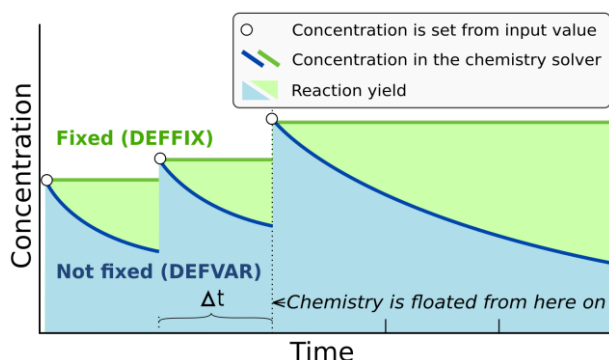
Figure 3: Schematic example of the effect of defining a compound in DEFFIX or DEFVAR. In this example, the variable is set by the user (in the GUI, this is done in the tab Time dependent input). The solid lines show the concentrations inside the chemistry solver for a compound which is fixed (green curve), and not fixed (blue curve). The circular symbols show the set concentration in each time step. The shaded areas represent the proportional impact of DEFFIX and DEFVAR on the concentrations of the reaction products of the compound. Depending on the model time step Δt, the differences can be substantial, and illustrates why the precursors should be set fixed, unless the chemistry needs to be floated.

2.2 Particle size distribution (PSD)

The main use of ARCA, besides simulating chemical reactions in the gas phase, is to compute the evolution of a population of aerosol particles experiencing dynamical processes such as coagulation, deposition and phase transition. There are many ways to formally approach this task, discussed e.g., by Whitby and McMurry (1997). In the atmosphere, the number of condensing species, different particle sizes and compositions is unlimited, and the practical mathematical descriptions of the PSD therefore require simplifying assumptions. The aerosol dynamics models are often characterized by their representation of the PSD. Typical representation types are the discrete, the spline, the sectional, the modal and the monodisperse representation.

In the discrete representation, particles have a discrete size and composition. That is, one size section includes exactly one discrete particle composition, given by the exact numbers of molecules of different compounds in the particle. This approach must be used when explicitly modelling initial cluster formation but gets increasingly complex and numerically heavy when more 'building blocks' are added, such as chemical compounds or particle sizes. ARCA's nucleation module consists of ACDC model which uses discrete representation.

Sectional models decrease complexity of the system by grouping parameters, and typically the particle diameter range (and equivalently volume, mass and surface) is divided into a limited number of intervals, or size bins. Particles in each bin have the same properties. This is a common approach in atmospheric modelling, however, its accuracy depends on the number of bins used and on the magnitude of change applied within one integration time step Δt. While large changes within Δt lead to a deviation from the analytical solution, small changes cause numerical diffusion especially when simulating condensational growth (Gelbard and Seinfeld 1980).

ARCA allows to choose between two sectional representations, the Fully Stationary (FS; Gelbard and Seinfeld 1980) method and the fixed grid moving average method (MA, also called 'moving centre sectional'; Jacobson 1997a). Future roadmap includes a hybrid method, discussed in section 6. The current representation methods are graphically summarized in Fig. 4.
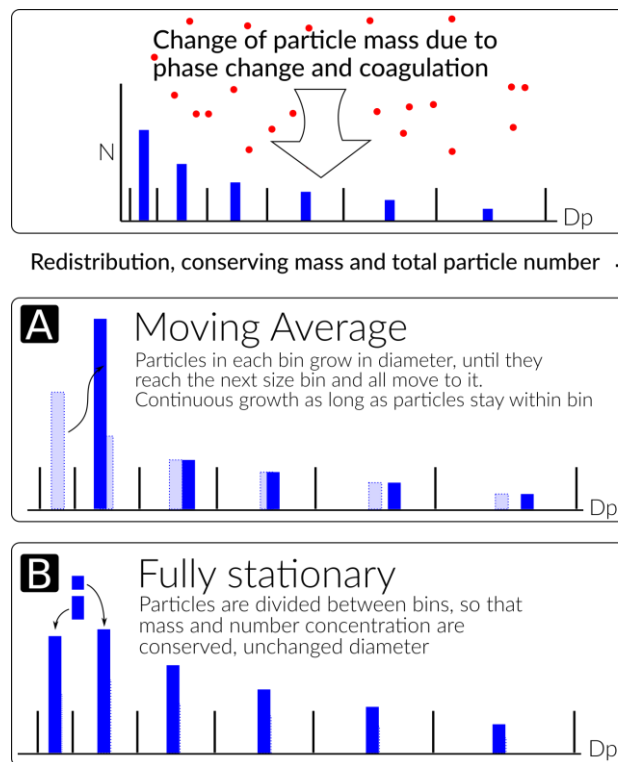
Figure 4: Schematic of the two particle size distribution representations, the fixed grid, moving average (MA, panel A) and the fully stationary (FS, panel B).

250

The FS method is very robust during computation but does not treat growth continuously, and therefore suffers from numerical diffusion (Jacobson 1997a). This is the result of the redistribution, where particles are assigned to bins below and above the actual size the particles have grown (or shrank), thereby introducing particles that are larger (or smaller) than the condensation or evaporation produces. In time this will lead to spreading of the size distribution, much like a diffusive process. The MA

method strongly reduces numerical diffusion as the particle diameter within the size grid can continuously change and particles are not distributed between bins. Main drawback of the MA method is the appearance of numerical artefacts, referred to as "pits" and "peaks", affecting the analysis of the results. However, they can be removed during data analysis by remapping the data on a new size grid as described by Mohs and Bowman (2011). Both PSD methods used conserve mass and total particle number.

The choice of the PSD representation does not affect the calculations in the aerosol dynamics module as they are separated from each other. This means that the different methods to represent PSDs can be changed or added without interfering the aerosol dynamics code. Aerosol related parameters, required to solve the dynamics, are provided by accessor functions (getters) and work for any PSD representation. Further, changes to the PSD by the dynamic processes are calculated in the aerosol dynamics module but applied in the PSD module. This allows further development of the scientific and computational aspects independently.

2.3 Initial new particle formation by molecular clustering

Formation of new particles from vapours by clustering of gas-phase molecules, often referred to as aerosol nucleation, is described by simulation of molecular cluster population dynamics with quantum chemistry input for cluster evaporation rates. This yields the formation rate of new particles per unit volume and unit time.

2.3.1 Molecular cluster dynamics simulation

Molecular cluster formation dynamics is solved by the ACDC code (https://github.com/tolenius/ACDC), which calculates the time-dependent cluster number concentrations for a given set of molecular clusters and ambient conditions. A detailed description of ACDC can be found in (Olenius et al. 2013). Briefly, ACDC generates and solves the discrete, molecular-resolution general dynamic equation, also known as the cluster birth–death equation, considering all possible collisions and evaporations among the clusters and vapour molecules, ionization and recombination processes, and external cluster sinks. When a collision results in a cluster that is outside the simulated system, and its composition satisfies the defined stability criteria, it is considered stable enough to not re-evaporate (Olenius et al. 2013). These outgrown clusters constitute the formation rate of new particles.

By default, collision rate constants are calculated as hard-sphere collision rates for collisions between electrically neutral species, and according to dipole-moment and polarizability-dependent parametrizations for collisions between neutral and ionic species (by default from Su and Chesnavich (1982)). Evaporation rate constants are obtained from quantum chemical cluster formation free energies. Ionization and recombination of clusters and molecules occur by collisions with primary ionic species, which originate from galactic cosmic rays and radon decay and are assumed to have the properties of O_2^- and H_3O^+. Cluster scavenging sink is obtained from the particle population modelled by ARCA, with sink rates R_{sink} calculated according to $R_{\text{sink}} = CS_{\text{vapor}} \times (D_{\text{cluster}} / D_{\text{vapor}})^{-1.6}$, where D_{cluster} is cluster diameter, CS_{vapor} and D_{vapor} are the condensation sink and diameter of the monomer (H_2SO_4 is used as proxy), respectively (Lehtinen et al. 2007). CS_{vapor} can also be give as time dependent input (CONDENS_SINK), if the aerosol module is not in use. The user familiar with ACDC may also modify the rate constants and the settings for the inclusion of different cluster dynamics processes. In addition to the ARCA user manual, the interested reader is referred to the ACDC manual, available from the repository, and references therein.

2.3.2 Available cluster chemistries

The default ARCA has slots for five ACDC modules, which can be switched on and off individually. The current default implementation includes two separate clustering chemistries: H_2SO_4–NH_3 and H_2SO_4–DMA (dimethylamine), including electrically neutral, negatively and positively charged clusters. Cluster evaporation rates are in the default installation calculated from previously published quantum chemical data computed at the B3LYP/CBSB7//RICC2/aug-cc-pV(T+d)Z level

295   of theory (Olenius et al. 2013), but the user may switch to alternative systems, calculated with DLPNO-CCSD(T)/aug-cc-pVTZ//ωB97X-D/6-31++G** level of theory. The main reasons for applying the B3LYP//RICC2 data are that these cover large sets of cluster compositions including all charging states and performs reasonably well compared to laboratory experiments (Almeida et al. 2013); Kürten et al. 2016). However, cluster evaporation tends to be underpredicted and thus the formation rates can be considered upper-limit estimates. ARCA's procedures allow easy rebuilding of additional cluster

300   chemistries, if the user wants to apply new or updated data for the evaporation rates. ~~ARCA has~~Furthermore, the number of slots for ~~five~~ ACDC modules~~, but the number~~ can be increased from five with minor code modifications.

2.3.3 Coupling of cluster and aerosol dynamics

The cluster dynamics simulation is implemented by passing the input for the ambient conditions to the cluster formation routine at each model time step. The input includes concentrations of the clustering vapours, temperature, primary ion production rate

305   (if supplied by the user), and condensation sink of H_2SO_4 (from previous time step or CONDENS_SINK), used as reference molecular size for scavenging sink CS_{vapor}. The cluster formation routine solves the time evolution of the cluster concentrations for the given time step, using the concentrations from the end of the previous time step as initial values, and returns the number of new particles that grow out of the cluster regime during the time step. This is converted to new particle formation rate (by $R_{formation} = C_{out}/\Delta t$) and handed to main module. The newly formed particles are then distributed within the first model PSD

310   size bins in the diameter range of $[\min(d_p), 1.15 \times \min(d_p)]$, with weights calculated by

$$w_i = 0.5 exp(-0.7i), i = \{2 \ldots d\}, w_1 = 1 - \sum_{i=2}^{d} w_i, \tag{3}$$

where d is the index of the bin closest to diameter $1.15 \times \min(d_p)$. This somewhat arbitrary distribution is based on the assumption that some stable clusters result from collisions that would produce larger than the minimum stable cluster, and assigns about 75–85% of the newly formed particles to the first bin. The factor to calculate the upper diameter for the

315   distribution (by default 1.15) can be changed with NPF_DIST (e.g., set to 1). The user is responsible for selecting a suitable PSD size range so that the minimum size for the simulation closely matches the size of the outgrowing particles from the ACDC systems. In case the selected $\min(d_p)$ in the model is larger than outgrowing cluster from any of the ACDC subsystems, the model issues a fatal warning in the beginning of the run and terminates. If the outgrowing clusters are more than 10% larger than $\min(d_p)$, a (non-fatal) warning is issued in the first time step. The newly formed particles are assigned a general non-

320   evaporating particle composition (in the model called GENERAL).

ACDC has an option to calculate a steady-state formation rate, which corresponds to a time-independent situation where the cluster concentrations have relaxed to a steady state for the given ambient conditions. The steady-state option (ACDC_SOLVE_SS) must not be used for a dynamic atmospheric case where the conditions vary with time, and thus the formation rate depends on the immediate history of the conditions. Instead, steady state option is useful if the user wishes to run the cluster routine as a

325   stand-alone model and study the dependence of the steady-state formation rate on, for example, vapour concentration or temperature. In general, while the steady-state approximation is necessary for computationally heavier large-scale models, it may cause artefacts especially at low vapour concentrations or dynamic conditions. As an explicit cluster simulation is easily embedded in a box model such as ARCA, it is reasonable to not introduce such unnecessary potential error source.

2.4 Other options for new particle formation rate

330   In addition to the explicit cluster dynamics simulation, simplified formation rate parametrization can be used. Currently, a parametrization for new particle formation from H_2SO_4 and representative organic components is available. This option approximates the formation rate as a function of H_2SO_4 and user-defined set of organic compound concentrations. The choice of what organic compounds (or proxies for them) to include in the set is not unambiguous and is dependent on the active chemistry scheme and assumptions made by the user. Still, such parametrizations are commonly used to characterize empirical

observations of particle formation (e.g., Paasonen et al. 2010). While they do not correspond to an explicit time-dependent formation rate and may not include all independent ambient parameters which could affect the formation rate, they are useful for assessing the magnitude of particle formation through the given chemistry.

To compliment the formation rates and the parametrization, the model has also a time-dependent input variable NUC_RATE_IN. When multiple particle formation rates are calculated, either by different ACDC systems, additional parametrizations or NUC_RATE_IN, the total formation rate – used in the aerosol module – is the sum of all processes. The output files contain the total formation rate, and separately those from the ACDC systems. Furthermore, if applicable, the formation rates of electrically neutral and positively and negatively charged particles is also saved. It must be emphasized that the charging states refer solely to the charges of the outgrowing particles in ACDC, not to the formation mechanisms of the particles. For instance, newly formed neutral particles may originate – and often do originate (Olenius et al. 2013) – from ion-mediated processes, where small ions recombine and the product grows further as a neutral cluster.

2.5 Condensation and evaporation of organic vapours and sulfuric acid

Formation and evolution of either natural or anthropogenic aerosols are dependent on gas-to-particle phase transition via nucleation, condensation and evaporation (Tsang and Brock 1982; Wagner 1982) and further on coagulation (von Smoluchowski 1918; Fuchs 1964). In ARCA, the condensational growth of particles due to organic vapours and sulfuric acid is defined by their gas and particle phase concentrations and pure liquid saturation vapour pressures p_{sat} (sulfuric acid is treated as non-evaporating vapour with $p_{sat} = 0$). ARCA employs the mass conserving, Analytical Predictor of Condensation (APC) scheme (Jacobson 1997a; Jacobson 2002), describing the condensational transfer of a gas phase compound q onto particles in size bin i, as the change in particle phase composition $c_{q,i}$, in a time interval Δt:

$$\frac{dc_{q,i,t}}{dt} = k_{q,i,t-\Delta t}\left(C_{q,t} - S'_{q,i,t-\Delta t}C_{q,eq,t-\Delta t}\right) \tag{4}$$

where $C_{q,t}$ is the gas phase concentration of compound q at time t, $S'_{c,i,t-\Delta t}$ is the equilibrium saturation ratio of the condensing gas, $C_{q,eq,t-\Delta t}$ is the pure compound saturation vapour concentration over a flat surface and $k_{q,i,t-\Delta t}$ is the mass transfer rate between the gas phase and all particles of size i (Jacobson 1997a). The mass transfer rate $k_{q,i,t} = n_i 2\pi d_i D_{eff,q,i}$ [s^{-1}], where n_i is the number concentration of particles in size bin i, d_i is the diameter of the particle in size bin i, and $D_{eff,q,i}$ is the diffusion coefficient of compound q with particles of size in bin i (Jacobson, 1997b). The equilibrium saturation ratio is calculated using the Köhler equation, which combines both the Kelvin and solute effect. The Kelvin effect accounts for the changes in saturation vapour pressure over the particle due to surface curvature, with small particles having larger saturation vapour pressures. The solute effect, or Raoult's law, describes the change in saturation vapour pressures for an ideal solution with a mixture of compounds in the particle droplet. Overall, the equilibrium saturation ratio for a compound is obtained by multiplying the solute effect, expressed as the molar fraction of the compound and the Kelvin term:

$$S'_{q,i,t} = x_{q,i}exp\left(\frac{4\sigma_{q,p}m_q}{R_g d_i T_t \rho_{q,p}}\right) \tag{5}$$

where $x_{q,i}$ is the organic molar fraction of compound q in a particle of bin i, $\sigma_{q,p}$ is the pure liquid surface tension, m_q is the molar mass of the compound, R_g is the universal gas constant, T_t is the temperature at time t, $\rho_{q,p}$ is the liquid density of the pure compound q and d_i is the diameter of particle in bin i.

Forward Euler method is used to integrate equation (4) over incremental time steps Δt, giving the change in particle phase concentrations $\Delta c_{q,i,t+\Delta t}$. The noniterative solution to equation **Error! Reference source not found.** can be written as:

$$c_{q,i,t} = c_{c,i,t-\Delta t} + \Delta t k_{c,i,t-\Delta t}\left(C_{q,t} - S'_{q,i,t-\Delta t}C_{q,s,t-\Delta t}\right) \tag{6}$$

Equation **Error! Reference source not found.** relies on final gas concentrations $C_{q,t}$, which are constrained by the mass balance equation

$$C_{q,t} + \sum_{i=1}^{N_{bins}} c_{q,i,t} = C_{q,t-\Delta t} + \sum_{i=1}^{N_{bins}} c_{q,i,t-\Delta t} \tag{7}$$

where N_{bins} is the number of particle size bins. Combining equation **Error! Reference source not found.** with the mass balance equation **Error! Reference source not found.**, the change in mass composition is calculated, which is then passed to the particle redistribution module. The final particle composition $c_{q,i,t}$ at each time step is constrained between max(0, $c_{q,i,t}$) to prevent evaporation from exceeding the total mass existing in each particle size bin (Jacobson 1997b).

375   The most crucial factor governing the condensational growth in the APC scheme is the compound specific pure liquid saturation vapour pressure p_{sat}. The structures of all compounds originating from MCM are available as SMILES codes, and ARCA includes a tool that can be used to extract the temperature dependent p_{sat} information using the methods in the UmanSysProp (http://umansysprop.seaes.manchester.ac.uk~~) database. The tool converts the data~~), an online facility for calculating the properties of individual organic molecules, currently hosted at the University of Manchester. ARCA's tool

380 converts the data aquired from UmanSysProp to A and B parameters of the Antoine equation: $\log_{10}(P_{sat}) = A - B/T$, where p_{sat} is in atm and T is the temperature [K].

There are often orders of magnitudes discrepancies (ranging from 10^{-13}–10^{-5} atm) in the estimated pure liquid saturation vapour pressures of species when using different methods (Valorso et al. 2011). Therefore, ARCA includes two different files for saturation vapour pressures; one obtained using the methods described in Nannoolal et al. (2008) and another using the

385 EVAPORATION (Compernolle et al. 2011). The files include only those compounds whose $p_{sat} \leq 10^{-6}$ atm (at 293.15 K), as more volatile compounds have negligible contribution in particle growth. In both files, the saturation vapour pressures for HOM's originating from PRAM are calculated using the group contribution method SIMPOL (Pankow and Asher 2008). Kurtén et al. (2016) have shown that NANNOOLAL produces low estimates of saturation vapour pressure for multifunctional compounds due to the absence of hydro-peroxide or peroxy-acid group parametrizations. SIMPOL on the other hand, has

390 shown to be in better agreement with pure-liquid vapour pressures of multifunctional compounds calculated using COSMO-RS (Conductor-like Screening Model for Real Solvents) (Eckert and Klamt 2002; Kurtén et al. 2016). The EVAPORATION includes a limited number of peroxides and peroxy acids (Kurtén et al. 2016), and is shown to produce the most accurate estimation of p_{sat} for all compounds for which EVAPORATION is applicable (O'Meara et al., 2014). The user can always provide their own pure liquid saturation vapour pressure data (using the same file formatting: compound_name, A, B). The

395 GUI also contains a tool where the NANNOLAAL and EVAPORATION data can be filtered with some other threshold than 10^{-6} atm.

2.6 Coagulation of particles

Coagulation occurs when two particles collide and coalesce or form agglomerates, and results in the increase of mean particle

400 size and decrease of number concentration in the total particle distribution, while total mass is unaffected. As ARCA is primarily intended to be used within submicron size range, the only coagulation process considered is the Brownian (thermal) coagulation, caused by thermally induced random motion of particles. Models of Brownian coagulation have existed for over a hundred years, starting from the work by von Smoluchowski (1918). The coagulation equation (Seinfeld and Pandis 2016) is

$$\frac{\partial N_i(t)}{\partial t} = \frac{1}{2}\sum_{j=1}^{i-1} K_{j,i-j} N_j N_{i-j} - N_i \sum_{j=1}^{\infty} K_{i,j} N_j \; , i \geq 2 \tag{8}$$

405 where $K_{i,j}$ is the coagulation coefficient, or coagulation kernel, between particles of size i and j, with number concentration N. Coagulation coefficient K depends on the size of the particles and increases with the particle size difference. Derivation of coagulation coefficient is different in the free molecular, transition and the continuous regime, and the commonly used method

to account for this is the Fuchs Form of Brownian Coagulation Coefficient (Fuchs 1964; Seinfeld and Pandis 2016) which also accounts the coagulation efficiency, or sticking coefficient, the fraction of collisions that lead to coagulation, α_c (in ARCA the default ALPHA_COA=1). In general coagulation coefficients contain uncertainties and can be affected by factors which are not considered in the model, such as particle shape, hardness, electric forces (whether induced or by net charge). The thermal speed of nanosize particles is in the order of tens of meters per second, and the probability of succesful coagulation could differ substantially from 1.

Other coagulation processes, such as gravitational, turbulent or shear coagulation are not considered in ARCA. This simplification can be justified for submicron sized particles, for which they are two–three orders of magnitudes slower compared to Brownian coagulation (Seinfeld and Pandis 2016). If an estimation of the effect of these additional coagulation pathways is needed, they could be considered as additional loss terms and handled in loss module.

2.7 Losses of condensable vapours and particles

In chamber experiments, losses of gases and particles to the chamber walls have a large influence on the outcome – same is true for simulations. In ambient conditions losses are more complex and harder to measure, due to advection, vertical mixing and different deposition processes. For simulations in confined spaces such as in a reaction chamber, the losses can be parameterized to some extent. ARCA considers losses of gas phase compounds and particles in separate steps, as shown in Fig. 1. The compounds considered in the vapour wall loss module are the same set of organic compounds that are condensing on the particles. The wall loss is based on the theory proposed by McMurry and Grosjean (1985), and is a reversible process characterized by two reaction rates $k_{gas \to wall}$ and $k_{wall \to gas}$

$$\frac{dC_{q,g}}{dt} = -k_{gas \to wall} C_{q,g} + k_{wall \to gas} C_{q,w},$$
$$\frac{dC_{q,w}}{dt} = k_{gas \to wall} C_{q,g} - k_{wall \to gas} C_{q,w} \tag{9}$$

where $C_{q,g}$ and $C_{q,w}$ are the total concentrations of compound q in gas phase and wall, respectively. ARCA uses Fortran DVODE to solve equations 9 for each compound at each time step. Rate constant $k_{gas \to wall}$ is derived from kinetic gas theory assuming a well stirred chamber and is limited either by diffusion near the wall, or uptake by the wall itself (McMurry and Grosjean 1985)

$$k_{gas \to wall,q} = \frac{A_{ch}}{V_{ch}} \alpha_w \bar{v}_q \left(4 + \frac{\pi \alpha_w \bar{v}_q}{2\sqrt{(k_e D_q)}} \right)^{-1} \tag{10}$$

where A_{ch} and V_{ch} are the area and volume of the chamber, α_w the accommodation coefficient, $\bar{v}_q$ and D_q the average thermal speed and diffusivity of molecule of compound q, respectively, and k_e the eddy diffusion coefficient. α_w (ALPHAWALL) is a property of the chamber wall, whereas k_e (EDDYK) is a description of the turbulent conditions in the chamber. In general, we should assume that α_w is different for each compound, but herehowever, these are generally not known, and a constant value of 10^{-5} is used for all compoundsas a first estimate, following e.g. Matsunaga and Ziemann (2010) and Zhang et al. (2014). Similar to surface tension data, individual α_w (or correction factors to constant ALPHAWALL if set to negative) can optionally be set in the file which defines the pure liquid saturation vapour pressure data. The rate $k_{wall \to gas}$ is derived from a steady state equilibrium where $\frac{dC_{q,g}}{dt} = \frac{dC_{q,w}}{dt} = 0$ and $C_{q,g} = C_{q,sat}$, then

$$k_{wall \to gas} = k_{gas \to wall} \frac{C_{q,sat}}{C_{q,w,eqv}} \tag{11}$$

where $C_{w,eqv,q}$ is the equivalent mass concentration on the wall (Pankow 1994; Matsunaga and Ziemann 2010). It is assumed that the activity of compound q is always 1, rendering $C_{w,eqv,q}$ to a constant $C_{w,eqv}$ (CW_EQV). The value of $C_{w,eqv}$ is not known,

440   but the sensitivity to the loss of low volatility vapours is small above values ~1µmol/m³ (Zhang et al. 2014). The default $C_{w,eqv}$ = 40 µmol/m³, ~~corresponding~~corresponds to 10 mg/m³ for an organic molecule with a mass of 250 g/mol.

McMurry and Grosjean (1985) discussed the effect of α_w. In the limit of very small α_w, Eq. (10) can be reduced to $k_{gas\rightarrow wall,q} = \frac{A}{V}\frac{\alpha_w\bar{v}}{4}$ and the uptake of gases is then limited mostly by surface reactions. With increasing α_w, the uptake becomes diffusion-limited, finally reducing to $k_{gas\rightarrow wall,q} = \frac{2A}{\pi V}\sqrt{k_e D}$, the separating value for α_w which divides the two modes of uptake being

445   at $\alpha_w = \frac{8}{\pi}\frac{\sqrt{k_e D}}{\bar{v}}$.

Aerosol losses are considered as irreversible deposition, and the first order loss rates [1/s] can either be a constant value or read from a file as (time and) size resolved values (which will be linearly interpolated for model times and bin diameters). If the losses are not known, they can also be approximated using parametrization from Lai and Nazaroff (2000), which considers the different deposition velocities to upwards, downwards and vertical surfaces. The necessary input is the floor area, height

450   and the friction velocity of the chamber (CHAMBER_FLOOR_AREA, CHAMBER_HEIGHT and USTAR, respectively). The last is used to characterize the near-surface turbulent flow, and can be estimated from the air flow velocity in the chamber with Clauser-plot method (Bruun 1996), or treated as a fitting parameter. Fig. 5 shows the calculated loss rates in 10 m³ and 30 m³ chamber (heights 2 and 3 m, respectively) with three different setting for friction velocity. Whichever way is used to derive the loss rate $k_{dep,i}$, the number of particles lost from bin i, $\Delta N_{i,\Delta t}$, in time step Δt are calculated by

$$\Delta N_{i,\Delta t} = N_{i,t}\left(1 - exp(k_{dep,i}\Delta t)\right) \tag{12}$$

455   The model saves the mass composition of particles lost to walls (in kg/m³) as a cumulative sum. Since the vapour wall losses are reversible, the model saves the mass flux to and from the walls (in kg/m³/s, positive value indicates gas to wall flux), calculated as an average over the time interval for saving results.
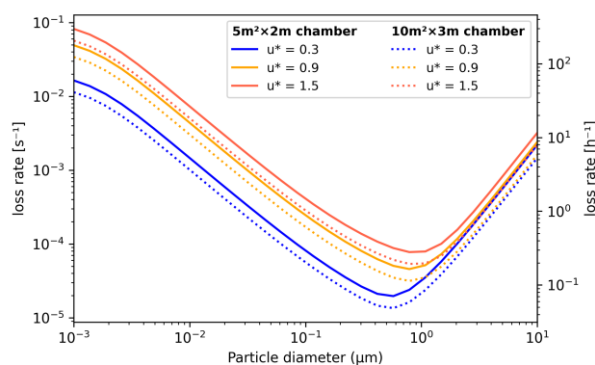
Figure 5: Particle loss rates as a function of particle diameter, friction velocity and chamber volume (given as floor area × height) as calculated by the aerosol loss rate parametrization. The rates are calculated at room temperature (20°C) and pressure (1 atm).

460

2.8 Model output

ARCA saves most of the output from the simulations in three compressed NetCDF4 (Network Common Data Form) files. The time resolution of the output can be defined in model seconds (FSAVE_INTERVAL), or as number of saved instances (FSAVE_DIVISION). The files contain time series of the environmental variables and nucleation rates and the names of the used

465   ACDC systems (*General.nc*), gas concentrations of the complete chemical set (*Chemistry.nc*) and aerosol number concentration, size, coagulation sink, particle growth (by condensation module) and loss rates, vapour concentrations in particle (size resolved) and gas phase and the vapour fluxes to and from the particle phase and walls (*Particles.nc*). All files

contain basic attributes of the model configuration, such as the name of the chemistry module used, user supplied description, name of the output directories and INITFILE, (real) date and time of the simulation.

470   When the model is run, a copy the INITFILE which was used to initialize the model is saved (*InitBackup.txt*). This file can be loaded in the GUI or used as such to repeat the simulation, provided that other input files are the same. Time series of particle number concentrations in normalized $\Delta N/\Delta(\log_{10}(d_p))$ and linear scale, and a list of condensing vapours is provided for convenience. If the model was run from the GUI, the screen output of the numerical model is also saved (*runReport.txt*). A complete list and description of the output variables and files is shown in Table 2.

475

Table 2: Description the output file contents, dimensions and units.

Variable name	Dimensions	Units	Description
All NetCDF files			
TIME_IN_SEC	time	s	Model time in seconds
TIME_IN_HRS	time	h	Model time in hours
General.nc			
[Time-dependent input variables]	time	[in units]	All Time-dependent input variables *which are used in the simulation,* are saved in the output after unit conversions, and it is good practice to check that the values are as intended.
J_ACDC_[1–5]_CM3	time, 4	s⁻¹ cm⁻³	Four elements are formation rates of summed, neutral, positively and negatively charged clusters ($J_{sum} = J_{neut} + J_{pos} + J_{neg}$).
J_ACDC_SUM_CM3	time	s⁻¹ cm⁻³	Summed total formation rates from all ACDC systems used
J_TOTAL_CM3	time	s⁻¹ cm⁻³	Summed total formation rates from all particle formation methods. This is the rate which is used in the aerosol module
CS_CALC	time	s⁻¹ cm⁻³	Condensation sink of sulfuric acid as calculated from the modelled PSD
Chemistry.nc			
[COMPOUND_NAMES]		cm⁻³	The full CH_GAS vector (CH_GAS is an internal variable containing concetrations of all chemical compounds in the chemistry
[REACTIVITIES] (if calculated)		s⁻¹	The effective reactivities (inverse lifetimes) of selected compounds, if defined in the chemistry
Particles.nc			
VAPOURS	composition		Names of the compounds that can go to particle phase. They are also listed in the text file CondensingVapours.txt.
NUMBER_CONCENTRATION	time, bins	cm⁻³	Particle number concentration. They are NOT normalized. Particle number concentration is also saved in two text files: Particle_conc.dat, which is exact copy of this variable, and Particle_conc.sum, which ARE normalised by $\Delta N/\Delta(\log_{10}(d_p))$. The text files contain time stamps in the first column and diameters in the first row. Additionally, the .sum-file contains the total particle concentration in the second column.
INPUT_CONCENTRATION	time, bins	cm⁻³	Particle number concentration of the input PSD (including the (multi)modal PSD), after it has been converted to model diameter grid. They are NOT normalized.
DIAMETER	time, bins	m	Particle nominal diameters
GROWTH_RATE	time, bins	nm/h	Instanteneous condensational growth rate of the particles. Positive = particles are growing. Note that this is not the same (even if it often is close) as what is obtained by appearance time or mode-fitting methods, when growth rate is calculated from observations.
COAG_SINK	time, bins	s⁻¹	Instanteneous sink of particles due to coagulation with larger particles
MASS	time, bins	kg	Particle mass
PARTICLE_COMPOSITION	time, bins, composition	kg	Singe particle mass, based on the volume. For the MA PSD method, this uses the actual particle diameter, not the nominal diameter.
MASS_FLUX_ON_PAR	time, composition	kg m⁻³ s⁻¹	Flux of vapours to the particles, averaged over FSAVE_INTERVAL. Positive = flux from gas phase to walls. Saved only if vapour wall loss module is used.
DEPOSITED_PAR_COMP	time, composition	kg m⁻³	Cumulative sum of composition lost to walls. Saved only if particle wall loss module is used.
PARTICLE_LOSS_RATE	time, bins	s⁻¹	Size-resolved instantaneous loss rate of particles. Saved only if particle wall loss module is used.

Variable name	Dimensions	Units	Description
MASS_FLUX_ON_WALLS	time, composition	kg	Flux of vapours to the chamber walls, averaged over FSAVE_INTERVAL. Positive = flux from gas phase to walls. Saved only if vapour wall loss module is used.

Other output files			
InitBackup.txt	-	-	Contains a backup of the INITFILE, and can be used to repeat the simulation
NMLS.conf	-	-	Dump of all namelist variables, even if they were not included in the INITFILE
Particle_conc.sum and .dat	time, bins	cm^{-3}	See NUMBER_CONCENTRATION
runReport.txt	-	-	The screen ouput of the numerical model. Only created when run from the GUI. From terminal *tee* command can be piped with the program call. The Create batch tool writes a bash script which has the *tee* command properly configured.
CondensingVapours.txt	-	-	See CONDENSABLES
optimization.txt	-	-	Output of the time step optimisation. Records the times and processes that were causing the time step increase or decrease.

3 Using the model – graphical user interface (GUI)

ARCA box has an extensive online user manual, (wiki.helsinki.fi/display/arca/ARCA+online+manual), along with tutorials of
installation and example cases. The manual is written completely from perspective of the user interface, and the underlying
scientific base of any procedure is mentioned only if relevant to the instruction. Therefore, we will here introduce the GUI
only broadly butwith a general notion of one possible workflow, and emphasize once more that the GUI is one of user who
wishes to learn to use the main features setting ARCA apart from other similar modelsmodel, should rely on the online user
manual. The manual allows the use of much more pictures, videos, interlinking between content and more informal addressing,
thus forming a vastly better pedagogical platform for learning than this paper could do.

Typically, a model such as ARCA is used for sensitivity studies and is run multiple times, changing various parameters. It is
very easy to lose track of the differences in different simulations, even when the simulation settings are not hardcoded. A user
interface is a valuable aid in organizing the model options in a way that helps the user to have a good visual control of the
workflow. Although a good user interface does not directly equal good science, we hope that it leads to better science. ARCA's
GUI enables this by showing the numerous simulation settings in the relevant context, thus making it easier to check that the
input (e.g., units, files, processes in use etc.) are correct, by automatizing file and directory naming and creation, by increasing
reproducibility with logging and automatic backup of executed simulation settings, by making inspection of the results
consistent with the plotting tools tailored for model output and by providing guidance with direct links to the corresponding
page in the online manual, just to name a few examples. While the numerical model is often run directly from the GUI, with a
valid INITFILE the compiled Fortran program can always be run from the command line, without the GUI. In fact, this is the
best way to use the model in batches of simulations, such as would often be done on a remotely run High Performance
Computer. (HPC).

3.1 GUI design principles

The primary principle of the GUI design has been that the numerical model is kept autonomous of the user interface. This
ensures that the model can be run on as many systems as possible, even when the user has no access to a graphical OS, such
as when working on an SSH connection to an HPC. Another aspect is that Fortran is a much more conservative language than
Python and it can be expected to work reliably as intended on each OS. While Python is cross-platform, it's reliance on multiple
extra packages and their rather quick updating schedule makes it more susceptible to introduce unintended behaviour in the
GUI. While such issues are usually fixed in the ARCA repository quite swiftly, it is highly convenient that the underlying

505 numerical model is working independently of the GUI. The independence between the model and the GUI is ensured through the INITFILE, where the GUI reads and writes a Fortran Namelist text file, which is used to initialize the numerical model. Another design principle has been that the GUI should allow further model development, that is, it should be able to write, save and read in any custom options, even if they are not yet fully incorporated in the graphical layout. Some of these options might be later incorporated, some may turn out to be unnecessary. This principle manifests itself in the GUI's tab *Custom*

510 *options*.

Third design principle has been to enable flexibility in the input to the model. All input is done via human readable text files. Not all modellers have their input data available in same units or time resolution, and the GUI lets the user to define theirs. However, this flexibility has limits and in the end the input files are expected to follow a certain structure which is covered in detail in the manual. Also the example files in the ModelLib directory can be used as a guide.

515 The last design principle is similar to what any graphical user interface typically aims to do: to collect the options of a program in meaningful groups and hierarchy, showing relevant and hiding unnecessary options, deriving information from user input such as parsing pathnames or calculating values, and provide assistance through help links or tool tips. It can be noted that while the amount of GUI options might seem intimidating, many of them are related to the way the input data is structured, and usually after the initial set up – which takes a while for the first time – the user can leave most options as they are and

520 concentrate on testing further with only a few key options.

3.2 Selected features of the GUI

To give an overview of the GUI, figures 56–78 show selected screenshots of the GUI window. For in-depth instructions and descriptions, the user is directed to the online manual, which contains an instructional video and transcript of setting up a simulation with the provided example files. To keep this work concise, here we give a general overview of the key points in

525 setting up a simulation. As an example, we have chosen the case which produces Fig. 11, and whose complete input is included in the directory ModelLib/Examples/APINENE_OXY. Figure 56a shows the tab *General options* (left panel), which contains many of the basic options for the simulation: naming of output, paths to input and output files, model time step, tool for creating batches of simulations and toggles for the main modules. The right panelBased on the choices in the "Modules in use", other tabs will be enabled or disabled, and the work procedure is to fill out the "forms" one tab at a time, and then use

530 "Run ARCA".

After *General options*, the most crucial set of options are in the next tab *Time dependent input* (Figure 6b). Here the concentrations of precursors and many environmental variables are defined. The logic in this tab is that any other input than temperature and pressure are optional. Any variable which is not defined here as an input, will have a constant 0 value. One picks the variables that are given as input to the model from the right-hand panel "Available input variables" and moves them

535 to selected list of input variables. Next, there are several options how to define the values of any variable. For example O_3 could come from measurements, in which case it would be read in from the ENV file from the column number defined in "Column/Link", or it could be a constant, in which case it would be sufficient to "Shift" the default value 0 by the constant amount, or we might want to multiply the measured values by a constant "Multi". Another option would be to link the concentration to some other variable, and then one would use that variable name in "Column/Link". Finally, there is a way to

540 use parametric input in the next tab "Parametric input", where a set of sliders can be used to create a smooth time series for any given input variable. This part of setting up the model is usually somewhat time consuming, but once properly done, the user can easily perform sensitivity tests by using the "Shift" and "Multi" options of any variable. Furthermore, the tool "Variations" can be used for sensitivity tests, which creates a batch of simulations where any given set of variables are varied within given ranges, containing all combinations of the different input settings.
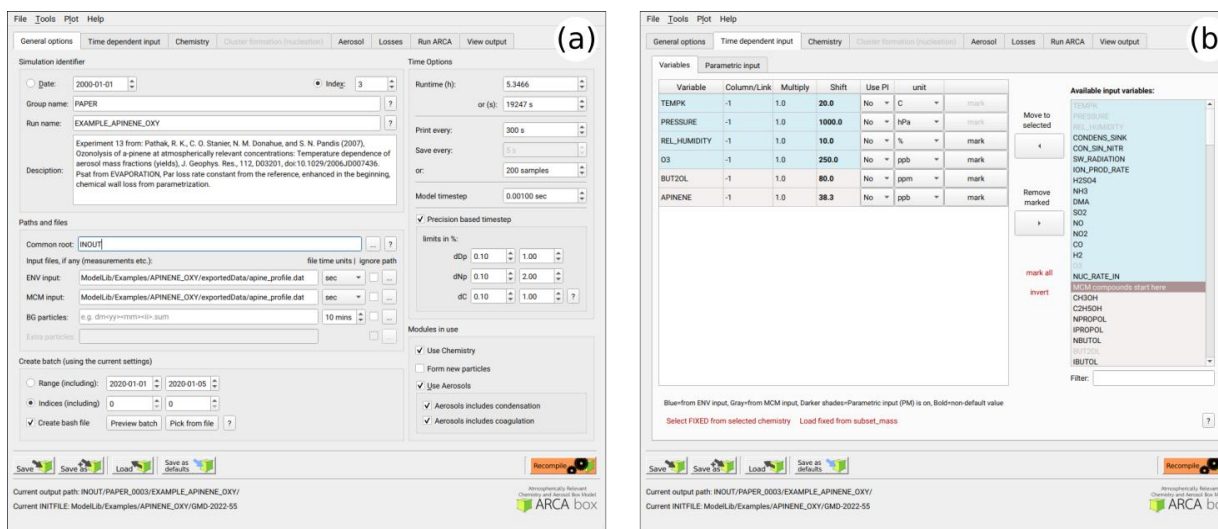
Figure 6: Screenshots of the GUI showing the tabs *General input* (a) and *Time dependent input* (b), where the model input concentrations and environmental variables are defined along with their sources and units. The settings shown here are from the simulation shown in Fig. 11.

Figure 7a shows the options related to aerosol module, such as size range and resolution of the PSD grid, its initialization with either measurements from file or using (multi)modal lognormal distribution, (as is done in this case), and duration and size range of initialization. ~~Figure 6 shows~~ This tab is also where the ~~input options for~~ pure liquid saturation vapour pressure properties are defined, in the "Vapour file" and optional "Vapour elemental composition" file. In our example case, a single mode log-normal particle size distribution was used to initialize the particles in the simulation. The (multi)modal PSD is defined by total particle number, mode diameter, standard deviation and relative contribution to the total PN. The GUI plots the resulting mode in real-time ~~dependent variables, and~~ and calculates total PM and particle area, as these are sometimes reported and can be used to fine-tune some unknown modal parameter such as the mode width.

Figure ~~Fig.~~7b shows an example of the model output during the runtime, when it is used from the GUI. The preferred way of setting up the model the first time is to start the model from the tab *Run ARCA* by pressing "Run model with current settings" and dealing with the eventual error messages, which might appear due to misconfiguration. If the model enter the main loop (after printing "Starting main loop"), it is advisable to press "Force stop" and read the initial report of the model that is printed in the "Monitor" window. If there are no warning messages, and the reported unit conversions and other reported behaviour corresponds to the intent of the user, the simulation can be performed in full.

Figure 8 shows examples of the output plotting tools such as surface plots (panel a) and particle mass and size distribution plots. (panel b). A useful tool is the *Live update* option, which shows the evolving particle size distribution surface plot during the simulation.
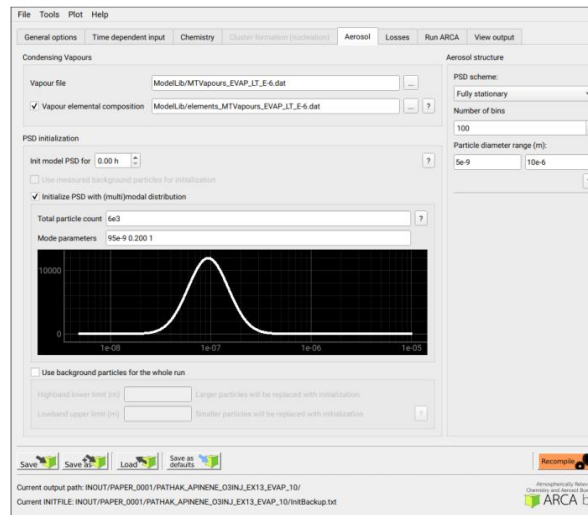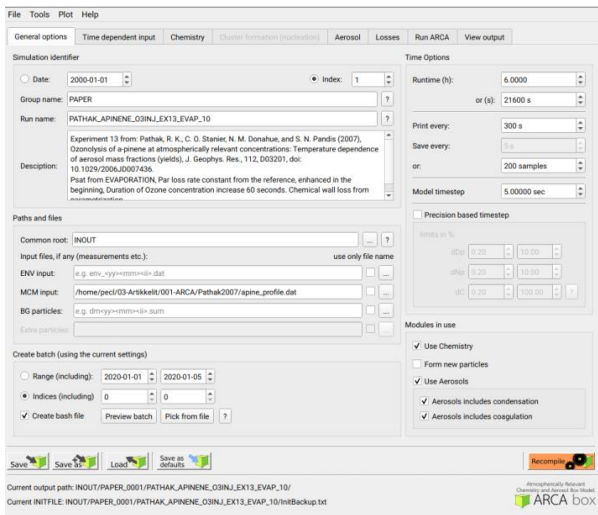
Figure 5: Screenshots of the GUI showing the tabs *General input* (left) and *Aerosol* (right), where the black plot is the user defined parametric initial particle size distribution that is distributed to the selected size bins. The settings shown here are from the simulation shown in Fig. 10.
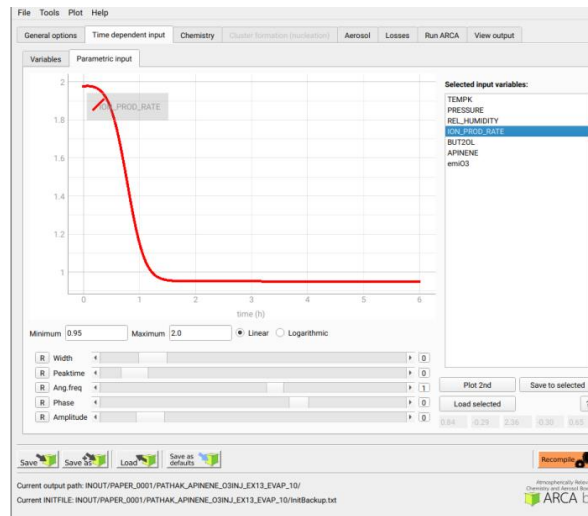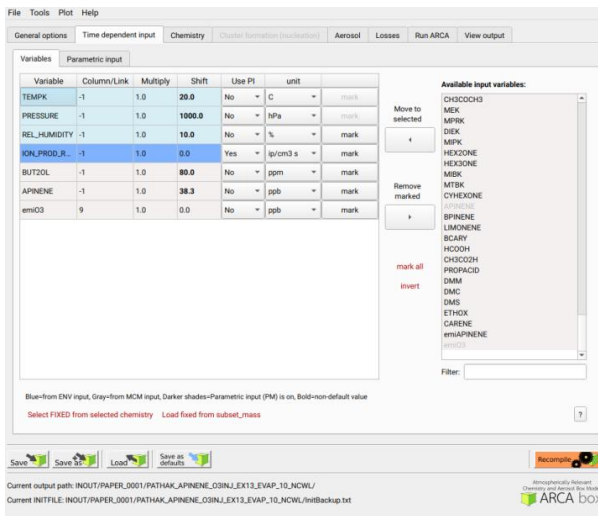
Figure 6: Example of the time dependent input definition: Selecting the necessary model input, their sources and units (left); parametric input tool (right).
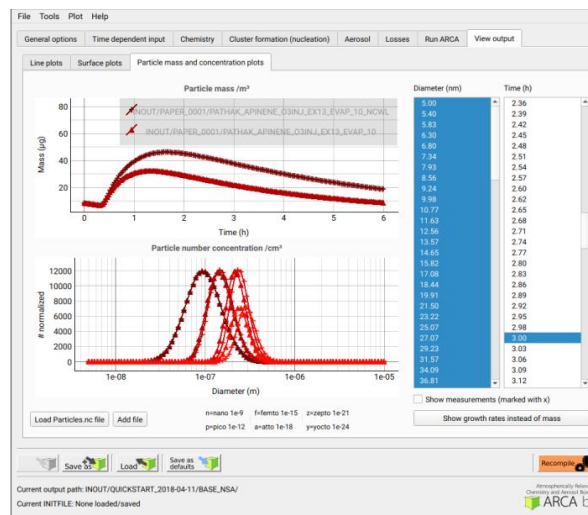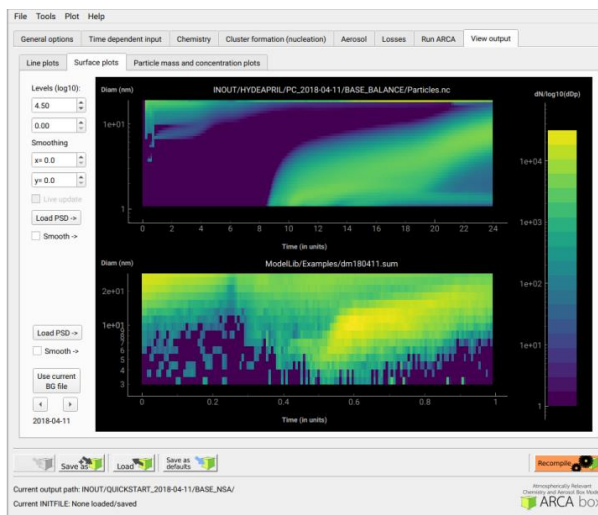
Figure 7: Examples of the plotting tools of the model output: surface plots of the modelled (left, top plot) and initialization PSD (left, lower plot); On the right comparison of two simulations, with total particle mass (right, top plot) and size distribution at three time instances (right, lower plot).

565
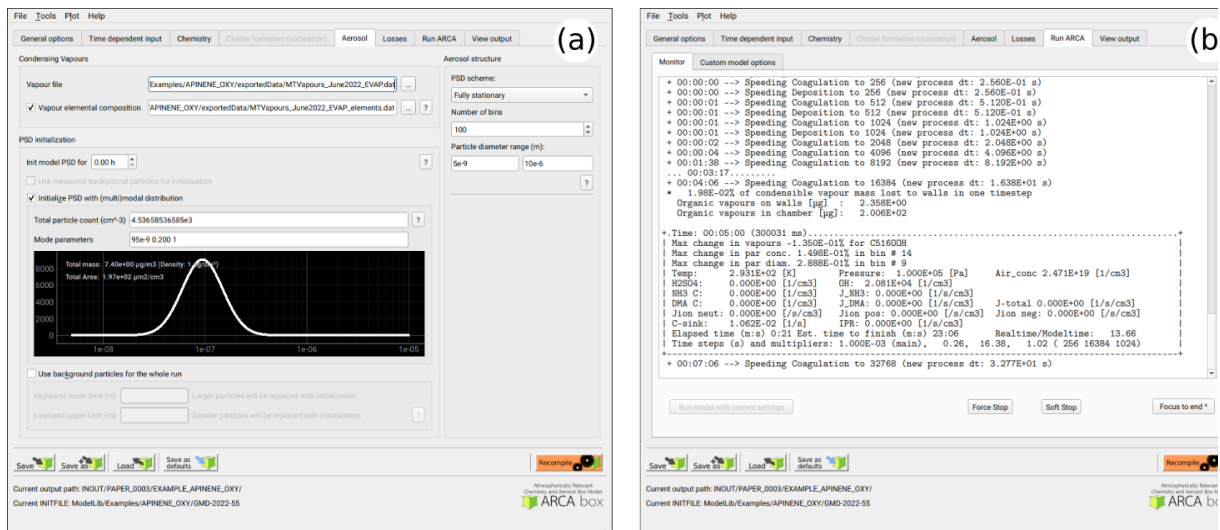
Figure 7: Options related to the discrete aerosol module; selection of PSD scheme, number of bins and the size range, and the parametric initial particle size distribution (panel a), and example of the model run-time output (panel b). The model can be stopped any time forcefully ("Force stop") or gracefully ("Soft stop"), where the latter saves the output gathered so far.
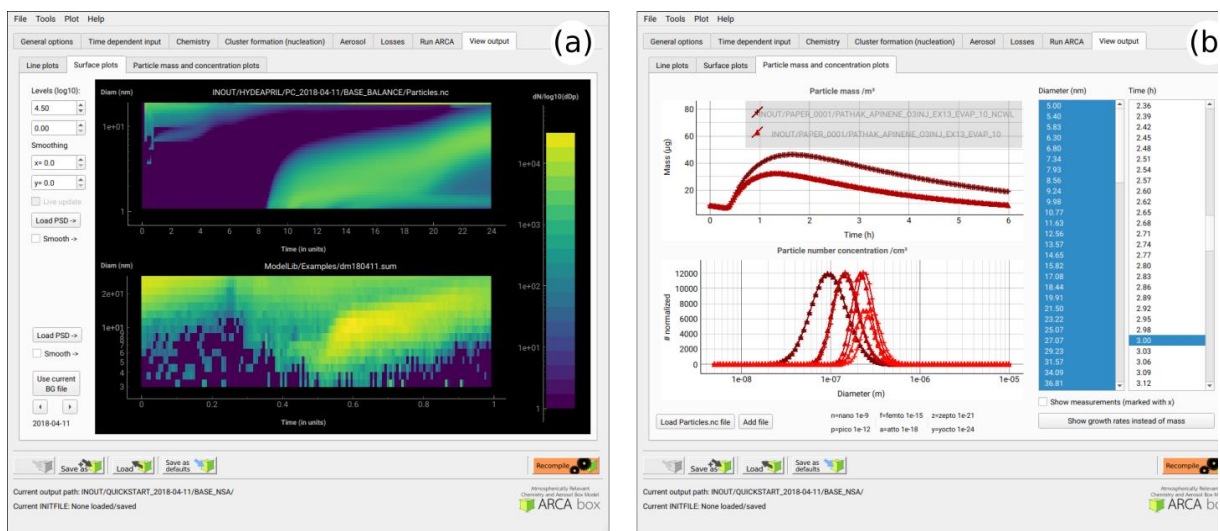
Figure 8: Examples of the plotting tools of the model output: surface plots of the modelled (left, top plot) and initialization PSD (left, lower plot); On the right comparison of two simulations, with total particle mass (right, top plot) and size distribution at three time instances (right, lower plot).

4 Verification and evaluation of main modules

570 The aim of this section is to verify that the modules in ARCA box perform programmatically as intended. We must stress that the validity of the results of any model is strongly dependent on the input parameters used. Here the reader is reminded of the most crucial parameters in addition to the user supplied concentrations:

– for the chemistry module the chemical reaction sets (and accompanying kinetic rate coefficients), spectral data

– for the formation rate module (ACDC) the Gibbs free energies

575 – for condensation and vapour loss modules the pure liquid saturation vapour pressures

These are provided in the default ARCA installation as a working example, and while they are from published sources, they are not intended to be used in all conditions and locations. Instead, the user should use the tools in the GUI and online manual to collect and prepare their own set of input parameters and submodules, and justify their use based on their simulation conditions. The manual has detailed instructions on how to acquire and format the input data, construct a chemistry module

580 and update the ACDC systems. The tests shown here are simplified cases whose purpose is to show that the calculations in the model are done correctly. The last test is a comparison against a chamber experiment, which utilises nearly all the modules

and therefore connects all the individual processes. The settings used in this simulation is shown in Appendix C and serve as an example of an INITFILE.

4.1 ACDC

585 For any given cluster system, the formation rates in ACDC depend largely on the evaporation rates of the clusters, generally calculated from the input Gibbs free energies. Figure 89 shows formation rates calculated with the four ACDC simulation systems, two for H_2SO_4–NH_3 and two for H_2SO_4–DMA. The systems calculated with the RICC2 (RICC2/aug-cc-pV(T+d)Z//B3LYP/CBSB7) method are described in Olenius et al. (2013) and can be found from the ACDC repository (github.com/tolenius/ACDC). The DLPNO level NH_3 system (DLPNO-CCSD(T)/aug-cc-pVTZ//ωB97X-D/6-31++G**) was

590 used in Besel et al. (2020), whereas the DLPNO DMA system was used in Myllys et al. (2019). Figure 89a shows the significance of ion-mediated clustering in the H_2SO_4–NH_3 system, as is apparent when comparing the total formation rates with and without the presence of ions. It also underlines the already mentioned notion that the charge of the outgrowing clusters does not necessarily correspond their pathway inside the system. The H_2SO_4–DMA cluster formation (Fig. 9b) shows weaker sensitivity to the presence of ions.

595
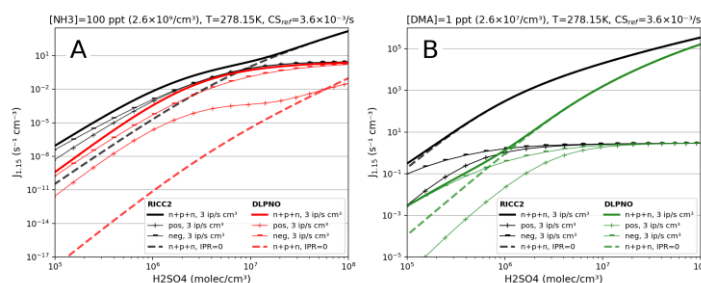
Figure 8: Steady-state particle formation rates from the two H_2SO_4–NH_3 (panel A) and two H_2SO_4–DMA systems (panel B). Both chemistries include data from RICC2 and DLPNO level of theories. Thick lines show the total formation rate, solid lines are in the presence of ions, dashed lines without ions present. All simulation used the same temperature (5° C) and external cluster losses (3.6×10⁻³/s).
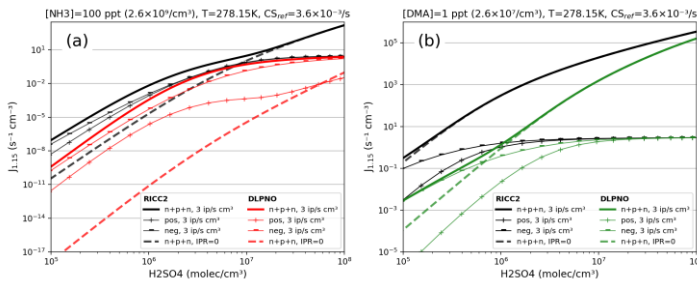
Figure 9: Steady-state particle formation rates from the two H$_2$SO$_4$–NH$_3$ (panel a) and two H$_2$SO$_4$–DMA systems (panel b). Both chemistries include data from RICC2 and DLPNO level of theories. Thick lines show the total formation rate, solid lines are in the presence of ions, dashed lines without ions present. All simulation used the same temperature (5° C) and external cluster losses (3.6×10⁻³/s).

4.~~3~~2 Verification of the coagulation module

The calculations of the Brownian coagulation module were verified in two parts. Figure ~~9~~10a shows the size dependant coagulation coefficients calculated by ARCA (for comparison, see figure 13.5 in Seinfeld and Pandis (2016)) whereas Fig. ~~9~~10b compares the evolution of a particle size distribution with an analytical solution to the Brownian coagulation of a polydisperse particle volume distribution. The solution applies constant, size-independent coagulation coefficient 10^{-9}/cm³/s (defined by the initial concentration $N_0 = 10^6$/cm³ and characteristic time $\tau_c = 2000$ s), and for this test ARCA's calculated coefficients were replaced with the same constant coagulation coefficient (for comparison, see figure 13.6 in Seinfeld and Pandis (2016)). Fig. 10 shows that on one hand the coagulation kernel is calculated in the same way as the in source, but also that the coagulation losses are correctly applied, and therefore the temporal evolution of the discrete particle size distribution in ARCA is identical with an analytical solution of the same initial size distribution.
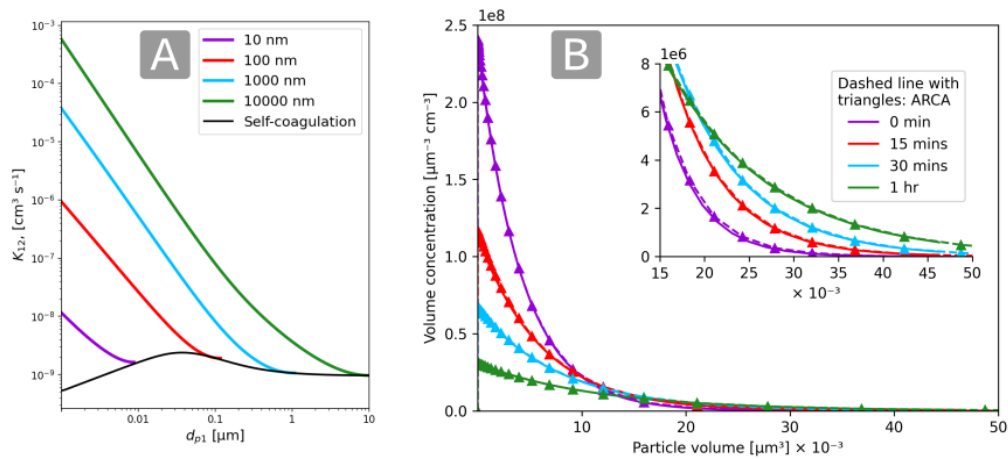
~~Figure 9: Coagulation coefficients used in ARCA box for four different particle diameters (panel A), with sticking coefficient α_s=1. Comparison with analytical coagulation solution (panel B).~~
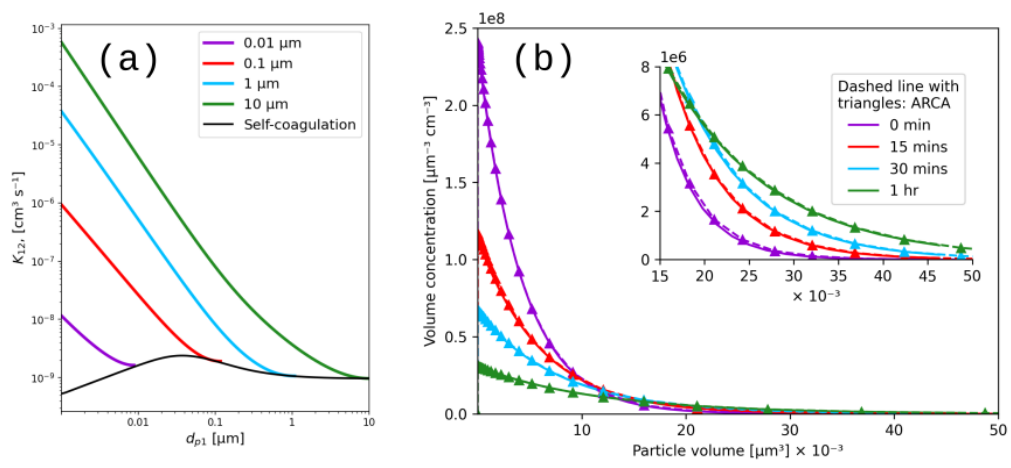
Figure 10: Coagulation coefficients used in ARCA box for four different particle diameters (panel A), with sticking coefficient α_g=1. Comparison with analytical coagulation solution (panel B).

4.~~2~~3 Chemistry, condensation and loss routines

We simulated α-pinene oxidation in high ozone and low OH chamber environment, similar as in experiment 13 in Pathak et al. ~~(2007).~~(2007) (Figure 11). The 10 m³ Teflon bag chamber was initially filled with seed particles, α-pinene and 2-butanol as OH scavenger. Then O_3 was introduced to the chamber. The reported mean particle loss rate (0.3/h) was expanded to size and time dependant profiles using Pierce et al. (2008), who measured the losses in the same chamber in more detail. ~~Figure 10 shows the resulting time series with~~They report an initially higher rate of loss in all their experiments, and attribute this to the growth of the particles (leading to slower average loss rate) and in the enhanced loss rate of initially charged seed particles. Since ARCA in its current form does not consider charge effects, we chose to use the reported loss rates, with higher initial rate. It means that the simulation is not showing the effect of the loss rate calculated by the particle loss module, but it does still verify that the rates are properly applied – given the good agreement in total particle mass time series. The simulation used moderate wall loss of condensing vapours (ALPHAWALL = 5×10^{-5}, CW_EQV = 40 µm/m³ and EDDYK = 0.05 s⁻¹). The final SOA mass yield of 0.~~168~~169 (final SOA mass / initial α-pinene mass) calculated by ARCA agrees well with the reported 0.17. Without evaporation from the particles, invoked by the accumulation of vapours to walls and the consequential supersaturation decrease, the calculated yield is 0.~~177.~~176. The final concentration of vapours deposited on the walls amounted to 13.4 µg/m³. In the chemistry scheme built for this test, ozone concentration was ~~regulated by emission rate (similarly as would be in a chamber experiment), and a mixing time of 1 minute was achieved by tuning the emission rate (in the end 2 ppb/s) so that the O_3 concentration increases from 0~~set to the target (250 ppb) ~~in about 200~~at time 1105 seconds, and was then ~~turned on only~~let evolve according to ~~keep~~ the ~~concentration constant~~chemical reactions. Without chemical wall loss the simulated yield is 0.286, overshooting the reported yield by a factor of 1.7. The pure liquid saturation vapour pressures used were derived using the EVAPORATION method. The chemistry was acquired from MCM and amended with the PRAM, and p_{sat} data was downloaded from UmanSysProp~~,~~ (umansysprop.seaes.manchester.ac.uk, Sect. 2.5), using the tools in ARCA box.

The ARCA distribution contains an example case which produces similar simulation than was used to produce Fig. 11. Here the initial time without ozone is omitted and the simulation starts immediately with 250 ppb concentration. To accommodate for the initial particle losses, the initial particle number concentration was set to 4537 cm⁻³. This simplification makes configuring the model much more straightforward, and produces the same result apart from the shift in time when compared with the experiment data.
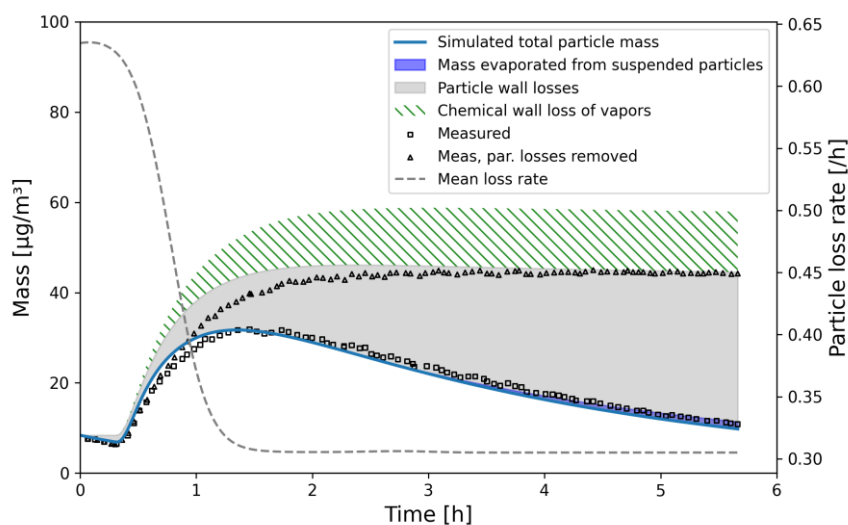
Figure 11: Comparison against α-pinene oxidation experiment (exp. 13, Pathak et al. 2007). Size-resolved aerosol wall losses were measured for the same chamber in Pierce et al. (2008). Moderate chemical wall loss is calculated with parametrisation from ARCA box using ALPHAWALL = 5×10⁻⁵, CW_EQV = 40 µm/m³ and EDDYK = 0.05 s⁻¹.

We also performed sensitivity runs where we tested the vapour wall parameters C_w and α_w. Changing C_w an order of magnitude lower and higher (to 4 and 400 µm/m³) changed the resulting yield to 0.179 and 0.166, and final total vapour mass on the wall was 7.16 and 16.46 µg/m³, respectively. For reasons discussed in section 2.7 about the limit of very small α_w, we saw no practical difference in the yield or vapour mass lost to walls after $\alpha_w > 10^{-4}$, where the uptake apparently has become diffusion-limited. The selected default value of α_w (5×10⁻⁵) can be considered to be close to the value where the surface reactions start playing a role on the uptake.

Table 3: Sensitivity of the vapour wall losses to parameters Cw and α_w.

	C_w [μmol/m³]	α_w [-]	Final yield [-]	Vapour concentration on walls [μg/m³]
Base case	**40**	**5×10⁻⁵**	**0.169**	**13.4**
$C_w \times 10$	400	5×10⁻⁵	0.166	16.5
$C_w \times 0.1$	4	5×10⁻⁵	0.179	7.2
$\alpha_w \times 0.1$	40	5×10⁻⁶	0.196	13.5
$\alpha_w \times 10$	40	5×10⁻⁴	0.164	13.3
$\alpha_w \times 100$	40	5×10⁻³	0.164	13.4

645

5 Technical information of ARCA box

5.1 Licensing

ARCA box is licensed under GPL 3.0, and the licensing statements (also those from auxiliary software) are included in the source code. The source code includes software that is not written by authors of ARCA, namely the Fortran ~~VODE~~DVODE

650 solver ("In the Public Domain", or IPD), ACDC (GPL 3) and KPP, which is not strictly necessary for ARCA but provided for convenience (GPL 3), as the original KPP is not able to compile very large chemistry schemes or long variable names.

5.2 System requirements

ARCA's numerical model is written in Fortran, and the user interface in Python 3. These environments must be installed and properly working on the computer. Also, since the output data is mainly saved in NetCDF 4 files, this software – along with

655 its Fortran and Python libraries must be installed prior to compilation and use. ARCA box has been developed on Linux platform, but due to the cross-platform nature of Python and the availability of Gnu Fortran for all three major OS's, the model has successfully been installed and used on all of them (on Windows GFortran is used through Cygwin and on MacOS through Xcode). The model has not been tested with Intel Fortran but as it is usually compatible with GFortran, we expect no major issues. The ARCA online manual has step-by-step instructions and videos for the installation of the prerequisite environments

660 as well as the model itself. It also contains solutions to installation problems which have been reported to us. After the necessary environments are working, installation and compiling the model itself is straightforward with the included Python installer script. The script will install the necessary Python packages (most importantly PyQt5, PyQtGraph, NumPy, Matplotlib and netCDF4) and compile the model.

5.3 Code availability

665 The ARCA model source code, described in this paper, is publicly accessible as a frozen archive (available at https://doi.org/10.5281/zenodo.~~6358578~~6787213). However, the most recent, constantly updated version is available for download upon request in www2.helsinki.fi/en/researchgroups/multi-scale-modelling/arca. The users are asked to provide their email address and a very brief overview of the intended field of study with ARCA. This information is used to inform of any future updates, fixes and other news regarding the model, as well as give the ARCA model development group information

670 of the different uses of the model. After the registration the user will be submitted a Git pull token to the private Gitlab repository. This token can be used later at any point for updating or reinstalling the code.

ARCA's user manual is in Wiki format, found in https://wiki.helsinki.fi/display/arca. There are also links from the GUI directly to the relevant parts in the online manual. In addition to the manual, there are tutorial videos, and troubleshooting instructions.

The manual is updated continuously as the model is further developed, but older states for previous versions are saved in pdf format, available for download at the site.

6 Future6 Current limitations and future developments

In its current state, we see ARCA as a robust base, a platform that packages established theories and knowledge of the central processes of this domain in a user-friendly and extendable program. Still, many known processes are for now omitted from the model, and the model will be developed further. This is aided by the fact that ARCA is one of the primary zero-dimensional process models used by the authors.

Current work with model development is concentrating on implementing an inorganic thermodynamic module, similarly as in ADCHEM and ADCHAM (Roldin et al. 2011; Roldin et al. 2014). This will enable calculations of size-resolved aerosol hygroscopic growth, acidity (pH) and the saturation concentrations of inorganic acids such as HNO_3, HCl and MSA (Methanesulfonic acid, CH_3SO_3H). This information will then be transferred to the condensation/evaporation module which will use the analytical predictor of dissolution (APD) method (Jacobson 1997b) to solve the gas-particle partitioning. The omission of particle phase chemistry (organic and inorganic) will affect the suitability of the model in marine air, where a considerable fraction of the aerosol mass is formed through oxidation processes which take place in aqueous phase (Xavier et al. 2022), and with very low concentrations of organic compounds the growth in the model would be almost solely based on the irreversible condensation of sulfuric acid which is formed in the gas phase chemistry, thus underestimating the total particle mass. Another major constituents of the secondary aerosol mass is nitric acid and ammonium, and these concentrations depend on the water content of the particles. One way to quantify in very broad strokes what a purely gas phase model is at worst missing would be to look at the measured aerosol composition around the world. Zhang et al. (2007) analysed the submicron aerosol AMS data from 37 field campaigns and found that organic compounds constitute on average 45 % (18–70%), sulfates 32% (10–67%), nitrates 10% (1.2–28%), ammonium 13% (6.9–19%) and chloride 0.6% (<D.L.-4.8%); the ranges in parenthesis are the range between different measurement locations. The current processes in the model are capable of bringing organic molecules, organic nitrates and sulfates (in the form of H_2SO_4 from SO_2 oxidation with OH) to the particle phase, but they would miss ammonium and chlorides. Some fraction of the nitrates and sulfates (and possibly organics too) are resulting from particle phase reactions in either aqueous form or oligomerization. The effect of particle phase oxidation of DMS and the subsequent formation of methanesulfonic acid (MSA) is one example of a process which is relevant over the oceans (de Jonge et al. 2021), but not necessarily a crucial omission over boreal forest, where similar approaches as in ARCA have been in good agreement with the measured particle mass and size distributions (Roldin et al. 2019).

Another area of improvement is the addition of charged particles, which is a significant factor in chamber wall losses., as was already discussed in Sect. 4.3. These extensions will be available after evaluation in the next version of ARCA. To compliment the current particle size distribution methods (FS and MA), we also plan to add a hybrid PSD representation (Chen and Lamb 1994; Pichelstorfer and Hofmann 2015). It consists of a fixed size bin grid where the concentrations are described by uniform distributions whose width can vary within each bin. Thus, upon growth or shrinkage, only a fraction of the population is moved to the neighbouring grid cell. This prevents numerical diffusion and avoids "pits" and "peaks" in the PSD output.

ARCA box has already been used and tested by several groups, and the feedback has helped further develop the model and its documentation. The approachable interface and model structure has been a great asset – on one hand it has helped to gain new users, and on the other hand it has helped us to improve the usability and stability, resulting to updates for the whole user community. We are looking forward to the future, where the users of ARCA further participate in the model development by sharing their experience, needs, ideas and even code additions.

Author contribution

PC and CX were the principal programmers and jointly coordinated the writing of the numerical model. PC wrote the user manual and the graphical user interface. LP wrote the PSD module and the time step optimization. PZ provided the chemistry modules and the supporting chemistry tools for the user interface. TO provided the ACDC plug-in. PR provided the loss routines. MB wrote the chemistry interface. All authors contributed to this manuscript by way of writing and commenting.

Acknowledgements

PC and CX share first authorship of this paper. We acknowledge the ACCC Flagship, funded by the Academy of Finland (grant number: 337549) and the computational resources from CSC – IT Center for Science, Finland. PC gratefully acknowledges the University of Edinburgh and University of Helsinki Partnership Programme on Forests. TO gratefully acknowledges the Swedish Research Council VR (grant no. 2019-04853) and the Swedish Research Council for Sustainable Development FORMAS (grant no. 2019-01433) for financial support. PR gratefully acknowledges the Swedish Research Council VR (grant no. 2019-05006), the Swedish Research Council for Sustainable Development FORMAS (grant no. 2018-01745), the Crafoord foundation (grant no. 20210969) and the strategic research area MERGE for financial support.

Competing interests

The authors declare that they have no conflict of interest.

Appendix A: List of variables used in the INITFILE

The user definable model options are briefly described here. **All options listed here can be defined in the graphical user interface (GUI)**. We want to emphasize that *there is no need to configure ARCA by manually editing the INITFILE.* In fact, this would probably lead to unintended outcomes, as some sanity checking of the options is done in the GUI. Additionally, the GUI contains tools, tooltips, help links and visualisation of the options. If necessary, for example for model development, the user can also insert any text input to the INITFILE from the GUI, and there is no need to part from the GUI workflow even when an option is not (currently) available in the GUI. All settings, even the raw input is always saved in the INITFILE written by the GUI, and will be available when an INITFILE is loaded in the GUI.

Table A1: Model variables which can be set from the GUI and INITFILE

Unit	Variable type	Variable name	Description, input options. **Bold** font shows the recommended value (if applicable)
NML_TIME			
h	REAL	RUNTIME	Duration of the simulation. The GUI accepts seconds and converts them to hours before writing the INITFILE. The simulation is always started from time 0, midnight, but the clock can be moved forward with NML_CUSTOM->START_TIME_S
s	REAL	DT	Integration time step. When USE_SPEED is TRUE, it is the minimum time step.
s	REAL	FSAVE_INTERVAL	Time interval (simulation time) for the output file writing
s	REAL	PRINT_INTERVAL	Time interval (simulation time) for the screen output
	INTEGER	FSAVE_DIVISION	when > **0**, the output files will contain approximately FSAVE_DIVISION timestamps
	CHARACTER	DATE	'yyyy-mm-dd', alternative to INDEX, used for naming directories and calculating solar angle.
	CHARACTER	INDEX	'xxxx' four digit index, alternative to INDEX, used when sun angle is not relevant.
NML_FLAG			
	LOGICAL	CHEMISTRY_FLAG	**T**/F whether chemistry module is used or not
	LOGICAL	CHEM_DEPOSITION	**T**/F whether vapour wall losses are considered
	LOGICAL	ACDC	**T**/F whether nucleation module (ACDC) is used or not. Does not affect parametric nucleation or formation rate that is sent in as time-dependent variable
	LOGICAL	ACDC_SOLVE_SS	T/**F** whether ACDC is solved to steady state
	LOGICAL	AEROSOL_FLAG	**T**/F whether aerosol module is used or not (nucleation module is unaffected)
	LOGICAL	CONDENSATION	**T**/F whether gas-particle partitioning is considered
	LOGICAL	COAGULATION	**T**/F whether aerosol coagulation is considered
	LOGICAL	DEPOSITION	**T**/F whether particle losses are considered
	LOGICAL	MODEL_H2SO4	**T**/F a convenience option, if T, H2SO4 concentrations are calculated by chemistry, if F, input values are used in all modules.
	LOGICAL	PRINT_ACDC	T/F if T, ACDC modules (in use) print on screen the cluster concentrations inside the system at each PRINT_INTERVAL
	LOGICAL	OPTIMIZE_DT	T/F whether time step optimization is used
	LOGICAL	ORG_NUCL	T/**F** whether parametrisation for organic nucleation is used
	LOGICAL	AFTER_CHEM_ON	T/**F** whether subroutine AFTER_CHEM in custom_functions.f90 is called after chemistry step. AFTER_CHEM is a dedicated injection point for customized code.
	LOGICAL	AFTER_NUCL_ON	T/**F** whether subroutine AFTER_NUCL in custom_functions.f90 is called after nucleation step. AFTER_NUCL is a dedicated injection point for customized code and is executed before total formation rate is applied in the aerosol module.
	CHARACTER	FILE_TIME_UNIT	'**day**','hrs','min','sec'. The time unit used in the input files for environmental, inorganic and organic variables.
	CHARACTER	LOSSFILE_TIME_UNIT	'**day**','hrs','min','sec'. The time unit used in the input files for the particle loss rate file.
NML_PATH			

	CHARACTER	INOUT_DIR	The root directory (relative to the executable, or absolute path) where data is saved. This must exist before starting the model
	CHARACTER	CASE_NAME	The directory which contains the runs (designated with RUN_NAME). These will be created by the model, and the DATE or INDEX will be appended to the path name. The GUI will always show the formatted output paths and provides quick access to the directory.
	CHARACTER	RUN_NAME	The name of the run directory, contained in CASE_NAME. When repeating similar simulations, where some variable(s) are changed, it is enough to change the RUN_NAME to create unique output data.

NML_PRECISION

%	REAL	DDIAM_RANGE	**0.5,3.0** two-element, comma-separated list for the optimized time step tolerances considering the change in the particle diameter dd_p
%	REAL	DPNUM_RANGE	**0.5,3.0** two-element, comma-separated list for the optimized time step tolerances considering the change in the particle number concentration dN_p
%	REAL	DVAPO_RANGE	**0.5,3.0** two-element, comma-separated list for the optimized time step tolerances considering the change in the vapour concentration dC

NML_VAP

	LOGICAL	USE_ATOMS	**T**/F whether elemental composition is used to calculate the diffusion diameter. If T, VAP_ATOMS must be provided.
	CHARACTER	VAP_NAMES	Path to file containing the pure liquid saturation vapour pressure data. The definition of which compounds condense on particles is based on the listed compounds in this file. Only the compounds that are found from the chemistry will be picked, so it is safe to have a larger set of compounds than actually exist in the chemistry. The compounds should be listed each on their own row, named exactly as in the chemistry, followed by molar mass, A and B term from the Antoine equation, as a *space separated* list. The GUI has a tool 'Create vapour file for aerosol module' which can extract the infdormation from UmansysProp with user supplied SMILES data. Example files are included in the default installation.
	CHARACTER	VAP_ATOMS	Path to file containing elemental composition of the organic compounds. This will be automatically created by the tool 'Create vapour file for aerosol module'. The file formatting follows the VAP_NAMES: a *space separated* list of compound name, molar mass, C, O, N, H, S, Cl, Br (where the chemical symbol is the number of each atom in the molecule).

NML_PARTICLE

	INTEGER	PSD_MODE	The method of PSD representation. **1** = Fully stationary (FS), 2 = Moving average, fixed grid (MA)
	INTEGER	N_BINS_PAR	Number of elements in the particle diameter grid
m	REAL	MIN_PARTICLE_DIAM	Minimum particle size
m	REAL	MAX_PARTICLE_DIAM	Maximum particle size. Should be large enough so that concentrations stay minimal as the boundary conditions are not constrained.
	CHARACTER	DMPS_FILE	Path to file containing the optional particle size distribution measurements. The time resolution is assumed to be 10 minutes, but can be changed in NML_CUSTOM→DMPS_TRES_MIN
h	REAL	DMPS_READ_IN_TIME	Time for initialization of the particle size distribution. The modelled particles are overwritten only in the times when there exists values in DMPS_FILE. The time resolution is assumed to be 10 minutes, but can be changed in NML_CUSTOM→DMPS_TRES_MIN. If (multi)modal PSD is used for initialization MMODAL_INPUT_INUSE = 1, the model PSD is replace every time step.
m	REAL	DMPS_HIGHBAND_LOWER_LIMIT	If USE_DMPS_PARTIAL is T, particles above this size continue being initialized even after DMPS_READ_IN_TIME.
m	REAL	DMPS_LOWBAND_UPPER_LIMIT	If USE_DMPS_PARTIAL is T, particles below this size continue being initialized even after DMPS_READ_IN_TIME.
	LOGICAL	USE_DMPS	**T**/F PSD will be initialized from DMPS_FILE, not from the Multimodal distribution.
	LOGICAL	USE_DMPS_PARTIAL	T/**F** If T, keeps overwriting the PSD at each DMPS_TRES_MIN, based on the sizes in DMPS_HIGHBAND_LOWER_LIMIT and DMPS_LOWBAND_UPPER_LIMIT. This feature is mostly used when accumulation mode particles are affected by transportation, which cannot be modelled in ARCA. For example, using a DMPS_HIGHBAND_LOWER_LIMIT of 2e-8, nucleation and early growth of particles below 20 nm can be simulated and still take into account the changes in the condensation and coagulation sink of the changing accumulation and Aitken mode. Can be terminated before the simulation with END_DMPS_PARTIAL

	CHARACTER	MMODAL_INPUT	'3e-8 0.15 0.5 1e-7 0.25 0.3' (shown here only as an example; the correct values depend completely on the user) Space-separated list containing *n* modal parameters. Three parameters per mode are needed, and the the resulting PSD will be formed from *n*/3 modes. The parameters are geometric mean diameter GMD [m], standard deviation of the (Gaussian) distribution and the weighing factor, used to scale the mode against other modes. It is strongly recommended that the modes are build in the GUI, which shows real-time visualization of the complete PSD, along with the total particle mass and area.
	REAL	N_MODAL	The total particle number concentration of the (multi)modal distribution [cm^{-3}]
	INTEGER	MMODAL_INPUT_INUSE	-1/1 if -1, (multi)modal PSD is not used for initialization
min	REAL	dmps_interval	**10** Time resolution for the background particles file.

NML_ENV

	CHARACTER	ENV_FILE	Path to file containing the (optional) time-dependent input data of the environmental variables and inorganic gases. Can be same file as MCM_FILE. This file is a two-dimensional, space-separated text file, where first line can (and is strongly recommended to) be a header, starting with #. Column 1 is time, and the following columns contain the values for the variables. Each line corresponds to a timestamp, and the times need not be with equal intervals. The time unit is by default day, but can be changed with FILE_TIME_UNIT. The column numbers link the data to the variable, and this is best done in the GUI. The units of the values must correspond to the ones shown in MODS(i)%UNIT, see below in NML_MODS, and are defined in the GUI. Same column can be linked to multiple variables, as they can be additionally modified using the MODS(i)%SHIFT and MODS(i)%MULTI. The GUI has a tool to print the header of the file to help in assigning the data to the model. If the time series of a variable is linked to another variable, this can be done in the GUI by using the variable name instead of the column number. The unit of the linked variable will be defined by the source variable, but the linked variable can be further modified with MODS(i)%SHIFT and MODS(i)%MULTI.
[s^{-1}]	CHARACTER	LOSSES_FILE	Path to file containing the (optionally time and) size resolved aerosol loss rates, using similar formatting The size and time space will be *linearly* interpolated. A constant time and size independent loss rate can be given by writing the value with prefix '#', for example, #0.003 will result in 0.003/s loss rate.
m²	REAL	CHAMBER_FLOOR_AREA	Chamber floor area, used in the wall loss parametrizations.
m	REAL	CHAMBER_HEIGHT	Chamber height, used in the wall loss parametrizations.
1/s	REAL	EDDYK	**0.05** Coefficient of eddy diffusion, describes turbulence in the chamber
m/s	REAL	USTAR	**0.05** Chamber friction velocity, affects particle wall losses
-	REAL	ALPHAWALL	**10e-5** Wall loss accommodation coefficient, wall/component property, assumed constant
mol/m³	REAL	CW_EQV	**40e-6** Equivalent mass concentration of the wall, equilibrium wall vapour concentration
[], or W m^{-2} nm^{-1}	CHARACTER	SPECTRUMFILE	Path to the file containing spectral data. The GUI accepts same wildcards in naming as ENV_FILE.
	LOGICAL	SWR_IS_ACTINICFLUX	T/F If T, actinic flux (AF) function is omitted and spectral irradiance is treated as AF. The integral of the product of spectral function and SW_RADIATION must produce AF in W/m²
nm	REAL	SWR_IN_LOWER	These define the range (band) of the pyranometer used for short wave irradiance measurement, and is only needed if the default sea level spectrum is used.
nm	REAL	SWR_IN_UPPER	

NML_MCM

	CHARACTER	MCM_FILE	Path to file containing the (optional) time-dependent input data of the organic precursor molecules. Can be same file as ENV_FILE. For formatting information, see ENV_FILE.

NML_ACDC

	CHARACTER	ACDC_SYSTEMS	1,1,0,0,0 comma-separated vector, 1=system in use,0=not in use
	CHARACTER	ACDC_LINKS(1)	'A H2SO4 N NH3' string linking the ACDC monomers to ARCA gas names.
	CHARACTER	ACDC_LINKS(2)	'A H2SO4 D DMA' string linking the ACDC monomers to ARCA gas names.
	...		

NML_MISC

°	REAL	LAT	Latitude (decimal degrees) of the location for field simulation, used to calculate solar angle. Values > 0 are N.
°	REAL	LON	Longitude (decimal degrees) of the location for field simulation, used to calculate solar angle. Values > 0 are W.

	CHARACTER	DESCRIPTION	Maximum 1000 characters long description of the simulation. Should not include special characters.
	REAL	CH_ALBEDO	Ground albedo, used for calculating the actinic flux.

m	CHARACTER	GR_SIZES	'3e-9,10e-9,20e-9' String defining the diameter ranges used to calculate the instantaneous condensational growth rate, averaged over the size ranges. Smallest particle size is always added in the calculation. Only used in the screen output, as the output files calculate size resolved growth rates. The example would produce following screen output at each PRINT_INTERVAL (the values are examples):
			`| Sizes: 1.1 --> 3.0 --> 10.0 --> 20.0 [nm]`
			`| GR: 1.56E-04 1.26E-04 1.50E-04 [nm/h]`

NML_CUSTOM

	LOGICAL	USE_RAOULT	**T**/F when T, use Raoult's law, the solute effect to the saturation concentration. Should generally always be T.
~~min~~	~~REAL~~	~~DMPS_TRES_MIN~~	~~**10** Time resolution for the background particles file.~~
sec	REAL	START_TIME_S	**0** If > 0, the simulation clock will be set to this time when the integration loop starts. By default the simulation clock starts at oo:oo (midnight). A caveat is that if background aerosols are initialized for example for 1 hour, and start_time_s>3600, there will be no initialization for particles. If the initialization is set to 2 hours, particles are constrained one hour. The model assumes that the input files still start at time zero (specifically, the first time stamp is subtracted from the time vector). Therefore, if the input data must contain some values at midnight, it is sufficient to have a row of zeros (one in each column) in the beginning of the input file (after the header).
	REAL	DMPS_MULTI	**1e6** The conversion factor to convert the number concentration values in the background particle file from particles/cm³ to particles/m³.
	CHARACTER	INITIALIZE_WITH	Path to a similar simulation which is used as initialization for the current run. Works only with constant time step.
	INTEGER	INITIALIZE_FROM	**0** Index to the place in the files used in the initialization. If 0, last value is used.
	REAL	VP_MULTI	**1.0** Factor for pure liquid saturation vapour pressures. Used for sensitivity test.
	INTEGER	LIMIT_VAPOURS	**0** if >0, only the first n compounds in the VAP_NAMES are taken to condense on particles
h	REAL	END_DMPS_PARTIAL	0 If >0, will terminate USE_DMPS_PARTIAL after this time (in simulation hours).
	LOGICAL	NO2_IS_NOX	T/**F** If T, NO$_2$ input is considered as NO$_X$. NO$_2$ concentration will be calculated inside the model by subtracting NO from NO$_X$.
	LOGICAL	NO_NEGATIVE_CONCENTRATIONS	**T**/F If T, all concentrations and environmental variables will be max(0,<input>) (T after it has been converted from °C to K)
h	REAL	FLOAT_CHEMISTRY_AFTER_HRS	Stops updating gas phase concentrations with input values after this time. Affects both concentrations and emissions
h	REAL	FLOAT_CONC_AFTER_HRS	Same as previous, but only for concentrations
h	REAL	FLOAT_EMIS_AFTER_HRS	Same as previous, but only for emissions
	LOGICAL	USE_RH_CORRECTION	**T**/F Use RH correction for H$_2$SO$_4$ condensation
s	REAL	DT_UPPER_LIMIT	**150.0,150.0,150.0** Three-element vector for the upper limits for the time steps CCH, COA and DEP, used with time step optimization.
	LOGICAL	ENABLE_END_FROM_OUTSIDE	**T**/F This option enables graceful termination of the simulation during the simulation. It is done by creating a file called ENDNOW.INIT in the output folder. The file must contain only one word STOP. If T, the existence of this file file is checked each time the model is in PRINT_INTERVAL. If found, the output files are finalized and the simulation stops. The procedure is a one-button operation in the GUI.
molec/cm³	REAL	MIN_CONCTOT_CC_FOR_DVAP	**1000** If time step optimization is used, the changes to control the time steps are not calculated for gases whose concentration is below this limit.
	REAL	ALPHA_COA	**1.0** sticking coefficient for coagulation
	LOGICAL	KELVIN_TAYLOR	T/**F** approximate Kelvin equation with first 2 terms of the Taylor series. Only used for comparison with some older models.
N/m², J/m³	REAL	SURFACE_TENSION	~~0.050~~**0.05** following Riipinen et al. (2010) Common surface tension for liquid phase organic compounds.
	CHARACTER	HARD_CORE	'**GENERIC**' Name of the non-evaporating generic composition, used for initialized particles and those from nucleation. Can be thought as primary particles. Must be the last item in the VAP_NAMES file.
kg/m³	REAL	ORGANIC_DENSITY	**1400** Common liquid phase density for organic compounds
kg/m³	REAL	HARD_CORE_DENSITY	**1400** Density of the GENERIC
	REAL	NPF_DIST	**1.15** multiplied with MIN_PARTICLE_DIAM to get the upper diameter where the nucleated particles are distributed. Majority of the clusters will be assigned in MIN_PARTICLE_DIAM.

NML_MODS

Note: MODS *is a vector of type (class)* input_mod, *used to store time dependent input data.*

INTEGER	MODS(i)%MODE	**0**/1 If 0, parametric function is not used. If 1, replace input by Parametric function, and then SHIFT and MULTI have no effect as the same result can be achieved with MIN and MAX.
INTEGER	MODS(i)%COL	**–1** Column number where the input data is read. –1 = data is not read from file. Column 1 is reserved for time.
REAL	MODS(i)%MULTI	**1.0** Multiplies the value of a variable, when it is obtained by reading a from input file or by linking to another variable. Has no effect if Parametric function is used
REAL	MODS(i)%SHIFT	**0.0** Shifts the variable value in the same units as defined in UNIT
REAL	MODS(i)%MIN	
REAL	MODS(i)%MAX	
REAL	MODS(i)%SIG	
REAL	MODS(i)%MJU	Parameters for the parametric input function. These should be modified using the GUI, which shows a visual output of the parametric function.
REAL	MODS(i)%FV	
REAL	MODS(i)%PH	
REAL	MODS(i)%AM	
CHARACTER	MODS(i)%UNIT	**Unit of the input, depends on the variable:** Temperature: `'K'`,`'C'` Pressure: `'Pa'`,`'hPa'`,`'mbar'`,`'kPa'`,`'bar'`,`'atm'` Relative humidity: `'%'` Condensation sink: `'1/s'` Short wave radiation: `'W/m2'` Ion production rate: `'ip/cm3 s'` Nucleation rate: `'1/cm3 s'` Concentrations, emissions: `'#/cm3'`,`'ppm'`,`'ppb'`,`'ppt'`,`'ppq'`
CHARACTER	MODS(i)%TIED	If given, will link one variable with another instead of using the column number.

Appendix B: Output files, variables and folder structure

Figure B1 shows how the output directory names are formed from the date or index, Case and Run names, and what files are written in the output directory. The directories are automatically created except for the Common Out (`INOUT_DIR`). NetCDF files are binary files and must be read with a compatible software. After installing ARCA the user has the necessary Python packages to access NetCDF (by 'import netCDF4'); other software includes ncdump, Octave, Panoply etc.
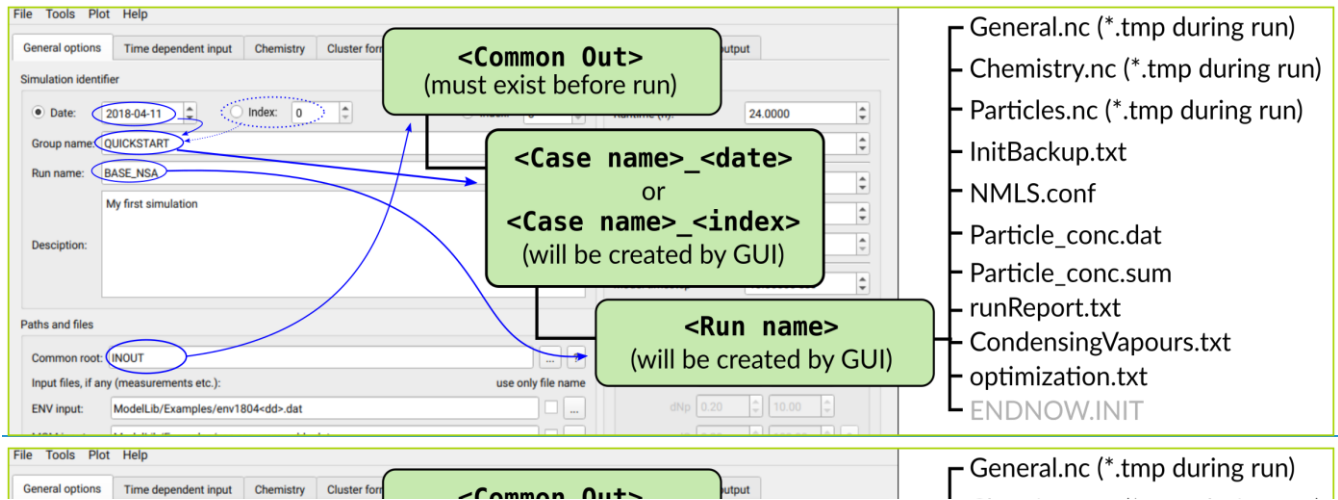
Appendix C: INITFILE

With INITFILE, the model can be run by loading it in the GUI: 1) by drag and drop 2) Ctrl-O or 3) 'Load settings', or run from terminal by giving the file path as command line option:

```
750    ./arcabox.exe path/to/INITFILE
```

Example INITFILE, used in simulation discussed in section 4.23

```
       # --------------------------------------------------
       #                 ARCA box setting file #1
755    #          Created at: Feb 23 2022, 13:08:10
       # --------------------------------------------------

       &NML_PATH
        INOUT_DIR = 'INOUT'
760    CASE_NAME = 'PAPER'
        RUN_NAME = 'FINAL_CW40'
       /

       &NML_FLAG
765    CHEMISTRY_FLAG = .TRUE.
        AEROSOL_FLAG = .TRUE.
        ACDC_SOLVE_SS = .FALSE.
        ACDC = .FALSE.
        CONDENSATION = .TRUE.
770    COAGULATION = .TRUE.
        DEPOSITION = .FALSE.
        CHEM_DEPOSITION = .TRUE.
        MODEL_H2SO4 = .FALSE.
        ORG_NUCL = .FALSE.
775    PRINT_ACDC = .FALSE.
        OPTIMIZE_DT = .TRUE.
        AFTER_CHEM_ON = .TRUE.
        AFTER_NUCL_ON = .FALSE.
       /
780
       &NML_TIME
        RUNTIME = 6.0
        DT = 0.001
        FSAVE_INTERVAL = 5
785    PRINT_INTERVAL = 300
        FSAVE_DIVISION = 200
        DATE = ''
        INDEX = '0003'
       /
790
       &NML_PARTICLE
        PSD_MODE = 1
        N_BINS_PAR = 100
        MIN_PARTICLE_DIAM = 5e-9
795    MAX_PARTICLE_DIAM = 10e-6
        N_MODAL = 6e3
        MMODAL_INPUT_INUSE = 1
        DMPS_FILE = ''
        EXTRA_PARTICLES = ''
800    MMODAL_INPUT = '95e-9 0.200 1'
        DMPS_READ_IN_TIME = 0.0
        DMPS_HIGHBAND_LOWER_LIMIT =
        DMPS_LOWBAND_UPPER_LIMIT =
        USE_DMPS = .FALSE.
805    USE_DMPS_PARTIAL = .FALSE.
       /

       &NML_ENV
        ENV_FILE = '/****/****/03-Artikkelit/001-ARCA/Pathak2007/apine_profile.dat'
810    SPECTRUMFILE = 'ModelLib/Photolyse/Spectra/swr_distribution.txt'
        SWR_IN_LOWER = 300
        SWR_IN_UPPER = 4000
        SWR_IS_ACTINICFLUX = .FALSE.
        LOSSES_FILE = 'INOUT/PAPER_0000/WALLLOSS/losses.dat'
815    CHAMBER_FLOOR_AREA = 5.0
        CHAMBER_HEIGHT = 2.0
        EDDYK = 0.05
        USTAR = 0.9
        ALPHAWALL = 5e-05
820    CW_EQV = 4e-05
       /

       &NML_MCM
        MCM_FILE = '/****/****/03-Artikkelit/001-ARCA/Pathak2007/apine_profile.dat'
825    /

       &NML_MODS
        MODS(1)   = 0 -1 1.00d+00 2.00d+01 1.00d+01  1.00d+05 2.340d0 12.000d0 0.000d0 0.000d0 1.000d0 'C' '' ! TEMPK
        MODS(2)   = 0 -1 1.00d+00 1.00d+03 1.00d+01  1.00d+05 2.340d0 12.000d0 0.000d0 0.000d0 1.000d0 'hPa' '' ! PRESSURE
830    MODS(3)   = 0 -1 1.00d+00 1.00d+01 1.00d+01  1.00d+05 2.340d0 12.000d0 0.000d0 0.000d0 1.000d0 '#' '' ! REL_HUMIDITY
        MODS(7)   = 1 -1 1.00d+00 0.00d+00 9.50d-01  2.00d+00 0.840d0 -0.28572d0 2.36d0 -0.30d0 0.65d0 '#' '' ! ION_PROD_RATE
        MODS(16)  = 0  6 1.00d+00 0.00d+00 1.00d+01  1.00d+05 2.340d0 12.000d0 0.000d0 0.000d0 1.000d0 'ppb' '' ! O3
```

```
      MODS(24)  = 0 -1 1.00d+00 8.00d+01 1.00d+01  1.00d+05 2.340d0 12.000d0 0.000d0 0.000d0 1.000d0 'ppm' '' ! BUT2OL
      MODS(151) = 0 -1 1.00d+00 3.83d+01 1.00d+01  1.00d+05 2.340d0 12.000d0 0.000d0 0.000d0 1.000d0 'ppb' '' ! APINENE
835 /

    &NML_MISC
     LAT = 60.0
     LON = -25.0
840  WAIT_FOR = 0
     DESCRIPTION = 'Experiment 13 from: Pathak, R. K., C. O. Stanier, N. M. Donahue, and S. N. Pandis (2007), Ozonolysis of
    a-pinene at atmospherically relevant concentrations: Temperature dependence of aerosol mass fractions (yields), J.
    Geophys. Res., 112, D03201, doi:10.1029/2006JD007436.<br>Psat from EVAPORATION, Par loss rate constant from the reference,
    enhanced in the beginning, Duration of Ozone concentration increase 60 seconds. Chemical wall loss from parametrization.'
845  CH_ALBEDO = 0.2
     GR_SIZES = ''
    /

    &NML_VAP
850  USE_ATOMS = .TRUE.
     VAP_NAMES = 'ModelLib/MTVapours_EVAP_LT_E-6.dat'
     VAP_ATOMS = 'ModelLib/elements_MTVapours_EVAP_LT_E-6.dat'
    /

855 &NML_ACDC
     ACDC_SYSTEMS = 0,0,0,0,0
     ACDC_links(1) = 'A H2SO4 N NH3'
     ACDC_links(2) = 'A H2SO4 D DMA'
     ACDC_links(3) = 'A H2SO4 D DMA'
860  ACDC_links(4) = 'A H2SO4 N NH3'
     ACDC_links(5) = 'A H2SO4 N NH3'
    /

    &NML_PRECISION
865  DDIAM_RANGE = 0.100000,1.000000
     DPNUM_RANGE = 0.100000,2.000000
     DVAPO_RANGE = 0.100000,1.000000
    /

870 &NML_CUSTOM
     FLOAT_CONC_AFTER_HRS = 0
     ORGANIC_DENSITY = 1400
     VP_MULTI = 1
     HARD_CORE_DENSITY = 1200
875  DT_UPPER_LIMIT = 30,70,70
    /

    &NML_FLAG
     FILE_TIME_UNIT = 'sec'
880 /

    # Following settings are for the GUI and not directly used by the model -----
    # RAW_INPUT = &NML_FLAG<br> FILE_TIME_UNIT = 'sec'<br>/
    #  INPUT_SETTINGS  =  'env_file:/****/****/03-Artikkelit/001-ARCA/Pathak2007/apine_profile.dat  mcm_file:/****/****/03-
885 Artikkelit/001-ARCA/Pathak2007/apine_profile.dat                dmps_file:                extra_particles:
    losses_file:INOUT/PAPER_0000/WALLLOSS/losses.dat        spectralFunctions:ModelLib/Photolyse/Spectra/swr_distribution.txt
    stripRoot_env:.FALSE. stripRoot_mcm:.FALSE. stripRoot_par:.FALSE. stripRoot_xtr:.FALSE.'
    # BATCH_SETTINGS = 'batchRangeDayBegin:2020-01-01 batchRangeDayEnd:2020-01-05 batchRangeIndBegin:0 batchRangeIndEnd:0
    indexRadioIndex:.TRUE. indexRadioDate:.FALSE. createBashFile:.TRUE. batchRangeDay:.FALSE. batchRangeInd:.TRUE.'
890 #-------------------------------------------------------------------------
```

References

Adams, P. J. & Seinfeld, J. H. (2002). Predicting global aerosol size distributions in general circulation models. *J Geophys Res*, 107, doi:10.1029/2001jd001010.

Akherati, A., He, Y., Coggon, M. M., Koss, A. R., Hodshire, A. L., Sekimoto, K., Warneke, C., de Gouw, J., Yee, L., Seinfeld, J. H., Onasch, T. B., Herndon, S. C., Knighton, W. B., Cappa, C. D., Kleeman, M. J., Lim, C. Y., Kroll, J. H., Pierce, J. R. & Jathar, S. H. (2020). Oxygenated Aromatic Compounds are Important Precursors of Secondary Organic Aerosol in Biomass-Burning Emissions. *Environmental Science &mathsemicolon Technology*, 54, 8568-8579, doi:10.1021/acs.est.0c01345.

Almeida, J., Schobesberger, S., Kürten, A., Ortega, I. K., Kupiainen-Määttä, O., Praplan, A. P., Adamov, A., Amorim, A., Bianchi, F., Breitenlechner, M., David, A., Dommen, J., Donahue, N. M., Downard, A., Dunne, E., Duplissy, J., Ehrhart, S., Flagan, R. C., Franchin, A., Guida, R., Hakala, J., Hansel, A., Heinritzi, M., Henschel, H., Jokinen, T., Junninen, H., Kajos, M., Kangasluoma, J., Keskinen, H., Kupc, A., Kurtén, T., Kvashin, A. N., Laaksonen, A., Lehtipalo, K., Leiminger, M., Leppä, J., Loukonen, V., Makhmutov, V., Mathot, S., McGrath, M. J., Nieminen, T., Olenius, T., Onnela, A., Petäjä, T., Riccobono, F., Riipinen, I., Rissanen, M., Rondo, L., Ruuskanen, T., Santos, F. D., Sarnela, N., Schallhart, S., Schnitzhofer, R., Seinfeld, J. H., Simon, M., Sipilä, M., Stozhkov, Y., Stratmann, F., Tomé, A., Tröstl, J., Tsagkogeorgas, G., Vaattovaara, P., Viisanen, Y., Virtanen, A., Vrtala, A., Wagner, P. E., Weingartner, E., Wex, H., Williamson, C., Wimmer, D., Ye, P., Yli-Juuti, T., Carslaw, K. S., Kulmala, M., Curtius, J., Baltensperger, U., Worsnop, D. R., Vehkamäki, H. & Kirkby, J. (2013). Molecular understanding of sulphuric acid–amine particle nucleation in the atmosphere. *Nature*, 502, 359-363, doi:10.1038/nature12663.

Besel, V., Kubečka, J., Kurtén, T. & Vehkamäki, H. (2020). Impact of Quantum Chemistry Parameter Choices and Cluster Distribution Model Settings on Modeled Atmospheric Particle Formation Rates. *J. Phys. Chem. A*, 124, 5931-5943, doi:10.1021/acs.jpca.0c03984.

Bird, R. E. & Riordan, C. (1986). Simple Solar Spectral Model for Direct and Diffuse Irradiance on Horizontal and Tilted Planes at the Earth's Surface for Cloudless Atmospheres. *J Clim Appl Meteorol*, 25, 87-97, doi:10.1175/1520-0450(1986)025<0087:sssmfd>2.0.co;2.

Boy, M., Hellmuth, O., Korhonen, H., Nilsson, E. D., ReVelle, D., Turnipseed, A., Arnold, F. & Kulmala, M. (2006). MALTE - model to predict new aerosol formation in the lower troposphere. *Atmos Chem Phys*, 6, 4499-4517, doi:10.5194/acp-6-4499-2006.

Boy, M. & Kulmala, M. (2002). Influence of spectral solar irradiance on the formation of new particles in the continental boundary layer. , , doi:10.5194/acpd-2-1317-2002.

Boy, M., Mogensen, D., Smolander, S., Zhou, L., Nieminen, T., Paasonen, P., Plass-Dülmer, C., Sipilä, M., Petäjä, T., Mauldin, L., Berresheim, H. & Kulmala, M. (2013). Oxidation of SO_2 by stabilized Criegee intermediate (sCI) radicals as a crucial source for atmospheric sulfuric acid concentrations. *Atmos Chem Phys*, 13, 3865-3879, doi:10.5194/acp-13-3865-2013.

Boy, M., Sogachev, A., Lauros, J., Zhou, L., Guenther, A. & Smolander, S. (2011). SOSA – a new model to simulate the concentrations of organic vapours and sulphuric acid inside the ABL – Part 1: Model description and initial evaluation. *Atmos Chem Phys*, 11, 43-51, doi:10.5194/acp-11-43-2011.

Bruun, H. H. (1996). Hot-Wire Anemometry: Principles and Signal Analysis. *Meas. Sci. Technol.*, 7, doi:10.1088/0957-0233/7/10/024.

Chen, J.-P. & Lamb, D. (1994). Simulation of Cloud Microphysical and Chemical Processes Using a Multicomponent Framework. Part I: Description of the Microphysical Model. *J. Atmospheric Sci.*, 51, 2613-2630, doi:10.1175/1520-0469(1994)051<2613:socmac>2.0.co;2.

Compernolle, S., Ceulemans, K. & Müller, J.-F. (2011). EVAPORATION: a new vapour pressure estimation method for organic molecules including non-additivity and intramolecular interactions. *Atmos Chem Phys*, 11, 9431-9450, doi:10.5194/acp-11-9431-2011.

935 Damian, V., Sandu, A., Damian, M., Potra, F. & Carmichael, G. R. (2002). The kinetic preprocessor KPP-a software environment for solving chemical kinetics. *Computers & Chemical Engineering*, 26, 1567-1579, doi:10.1016/s0098-1354(02)00128-x.

Eckert, F. & Klamt, A. (2002). Fast solvent screening via quantum chemistry: COSMO-RS approach. *AIChE Journal*, 48, 369-385, doi:10.1002/aic.690480220.

940 Fuchs, N. A. (1964). *The mechanics of aerosols*. : Pergamon Press, London.

Gelbard, F. & Seinfeld, J. H. (1980). Simulation of multicomponent aerosol dynamics. *J. Colloid Interface Sci.*, 78, 485-501, doi:10.1016/0021-9797(80)90587-1.

Jacobson, M. Z. (1997a). Development and application of a new air pollution modeling system—II. Aerosol module structure and design. *Atmos. Environ.*, 31, 131-144, doi:10.1016/1352-2310(96)00202-6.

945 Jacobson, M. Z. (1997b). Numerical Techniques to Solve Condensational and Dissolutional Growth Equations When Growth is Coupled to Reversible Reactions. *Aerosol Sci Tech*, 27, 491-498, doi:10.1080/02786829708965489.

Jacobson, M. Z. (2002). Analysis of aerosol interactions with numerical techniques for solving coagulation, nucleation, condensation, dissolution, and reversible chemistry among multiple size distributions. *J Geophys Res*, 107, doi:10.1029/2001jd002044.

950 Jacobson, M. Z. (2005). *Fundamentals of Atmospheric Modeling*. : Cambridge University Press.

Jenkin, M. E., Saunders, S. M. & Pilling, M. J. (1997). The tropospheric degradation of volatile organic compounds: a protocol for mechanism development. *Atmos. Environ.*, 31, 81-104, doi:10.1016/s1352-2310(96)00105-7.

Jenkin, M. E., Young, J. C. & Rickard, A. R. (2015). The MCM v3.3.1 degradation scheme for isoprene. *Atmos Chem Phys*, 15, 11433-11459, doi:10.5194/acp-15-11433-2015.

955 de Jonge, R. W., Elm, J., Rosati, B., Christiansen, S., Hyttinen, N., Lüdemann, D., Bilde, M. & Roldin, P. (2021). Secondary aerosol formation from dimethyl sulfide – improved mechanistic understanding based on smog chamber experiments and modelling. *Atmos Chem Phys*, 21, 9955-9976, doi:10.5194/acp-21-9955-2021.

Karl, M., Pirjola, L., Grönholm, T., Kurppa, M., Anand, S., Zhang, X., Held, A., Sander, R., Maso, M. D., Topping, D., Jiang, S., Kangas, L. & Kukkonen, J. (2022). Description and evaluation of the community aerosol dynamics model MAFOR v2.0.
960 *Geosci Model Dev*, 15, 3969-4026, doi:10.5194/gmd-15-3969-2022.

Kokkola, H., Kühn, T., Laakso, A., Bergman, T., Lehtinen, K. E. J., Mielonen, T., Arola, A., Stadtler, S., Korhonen, H., Ferrachat, S., Lohmann, U., Neubauer, D., Tegen, I., Drian, C. S.-L., Schultz, M. G., Bey, I., Stier, P., Daskalakis, N., Heald, C. L. & Romakkaniemi, S. (2018). SALSA2.0: The sectional aerosol module of the aerosol–chemistry–climate model ECHAM6.3.0-HAM2.3-MOZ1.0. *Geosci Model Dev*, 11, 3833-3863, doi:10.5194/gmd-11-3833-2018.

965 Kürten, A., Bianchi, F., Almeida, J., Kupiainen-Määttä, O., Dunne, E. M., Duplissy, J., Williamson, C., Barmet, P., Breitenlechner, M., Dommen, J., Donahue, N. M., Flagan, R. C., Franchin, A., Gordon, H., Hakala, J., Hansel, A., Heinritzi, M., Ickes, L., Jokinen, T., Kangasluoma, J., Kim, J., Kirkby, J., Kupc, A., Lehtipalo, K., Leiminger, M., Makhmutov, V., Onnela, A., Ortega, I. K., Petäjä, T., Praplan, A. P., Riccobono, F., Rissanen, M. P., Rondo, L., Schnitzhofer, R., Schobesberger, S., Smith, J. N., Steiner, G., Stozhkov, Y., Tomé, A., Tröstl, J., Tsagkogeorgas, G., Wagner, P. E., Wimmer,
970 D., Ye, P., Baltensperger, U., Carslaw, K., Kulmala, M. & Curtius, J. (2016). Experimental particle formation rates spanning tropospheric sulfuric acid and ammonia abundances, ion production rates, and temperatures. *Journal of Geophysical Research: Atmospheres*, 121, doi:10.1002/2015jd023908.

Kurtén, T., Tiusanen, K., Roldin, P., Rissanen, M., Luy, J.-N., Boy, M., Ehn, M. & Donahue, N. (2016). α-Pinene Autoxidation Products May Not Have Extremely Low Saturation Vapor Pressures Despite High O:C Ratios. *J. Phys. Chem. A*, 120, 2569-2582, doi:10.1021/acs.jpca.6b02196.

Kylling, A., Webb, A. R., Bais, A. F., Blumthaler, M., Schmitt, R., Thiel, S., Kazantzidis, A., Kift, R., Misslbeck, M., Schallhart, B., Schreder, J., Topaloglou, C., Kazadzis, S. & Rimmer, J. (2003). Actinic flux determination from measurements of irradiance. *J Geophys Res*, 108, doi:10.1029/2002jd003236.

Lai, A. C. K. & Nazaroff, W. W. (2000). MODELING INDOOR PARTICLE DEPOSITION FROM TURBULENT FLOW ONTO SMOOTH SURFACES. *J Aerosol Sci*, 31, 463 - 476, doi:https://doi.org/10.1016/S0021-8502(99)00536-4.

Lehtinen, K. E., Maso, M. D., Kulmala, M. & Kerminen, V.-M. (2007). Estimating nucleation rates from apparent particle formation rates and vice versa: Revised formulation of the Kerminen–Kulmala equation. *J Aerosol Sci*, 38, 988-994, doi:10.1016/j.jaerosci.2007.06.009.

Matsunaga, A. & Ziemann, P. J. (2010). Gas-Wall Partitioning of Organic Compounds in a Teflon Film Chamber and Potential Effects on Reaction Product and Aerosol Yield Measurements. *Aerosol Sci Tech*, 44, 881-892, doi:10.1080/02786826.2010.501044.

McGrath, M. J., Olenius, T., Ortega, I. K., Loukonen, V., Paasonen, P., Kurtén, T., Kulmala, M. & Vehkamäki, H. (2012). Atmospheric Cluster Dynamics Code: a flexible method for solution of the birth-death equations. *Atmos Chem Phys*, 12, 2345-2355, doi:10.5194/acp-12-2345-2012.

McMurry, P. H. & Grosjean, D. (1985). Gas and aerosol wall losses in Teflon film smog chambers. *Environmental Science & Technology*, 19, 1176-1182, doi:10.1021/es00142a006.

Mohs, A. J. & Bowman, F. M. (2011). Eliminating Numerical Artifacts When Presenting Moving Center Sectional Aerosol Size Distributions. *Aerosol Air Qual Res*, 11, 21-30, doi:10.4209/aaqr.2010.06.0046.

Myllys, N., Kubečka, J., Besel, V., Alfaouri, D., Olenius, T., Smith, J. N. & Passananti, M. (2019). Role of base strength, cluster structure and charge in sulfuric-acid-driven particle formation. *Atmos Chem Phys*, 19, 9753-9768, doi:10.5194/acp-19-9753-2019.

Nannoolal, Y., Rarey, J. & Ramjugernath, D. (2008). Estimation of pure component properties. *Fluid Phase Equilibr*, 269, 117-133, doi:10.1016/j.fluid.2008.04.020.

O'Meara, S. P., Xu, S., Topping, D., Alfarra, M. R., Capes, G., Lowe, D. & McFiggans, G. (2020). PyCHAM (v1.3.4): a Python box model for simulating aerosol chambers. , , doi:10.5194/gmd-2020-234.

Olenius, T., Kupiainen-Määttä, O., Ortega, I. K., Kurtén, T. & Vehkamäki, H. (2013). Free energy barrier in the growth of sulfuric acid–ammonia and sulfuric acid–dimethylamine clusters. *J. Chem. Phys.*, 139, 084312, doi:10.1063/1.4819024.

Ortega, I. K., Kupiainen, O., Kurtén, T., Olenius, T., Wilkman, O., McGrath, M. J., Loukonen, V. & Vehkamäki, H. (2012). From quantum chemical formation free energies to evaporation rates. *Atmos Chem Phys*, 12, 225-235, doi:10.5194/acp-12-225-2012.

Paasonen, P., Nieminen, T., Asmi, E., Manninen, H. E., Petäjä, T., Plass-Dülmer, C., Flentje, H., Birmili, W., Wiedensohler, A., Hõrrak, U., Metzger, A., Hamed, A., Laaksonen, A., Facchini, M. C., Kerminen, V.-M. & Kulmala, M. (2010). On the roles of sulphuric acid and low-volatility organic vapours in the initial steps of atmospheric new particle formation. *Atmos Chem Phys*, 10, 11223-11242, doi:10.5194/acp-10-11223-2010.

Pankow, J. F. (1994). An absorption model of gas/particle partitioning of organic compounds in the atmosphere. *Atmos. Environ.*, 28, 185-188, doi:10.1016/1352-2310(94)90093-0.

Pankow, J. F. & Asher, W. E. (2008). SIMPOL.1: a simple group contribution method for predicting vapor pressures and enthalpies of vaporization of multifunctional organic compounds. *Atmos Chem Phys*, 8, 2773-2796, doi:10.5194/acp-8-2773-2008.

1015 Pathak, R. K., Stanier, C. O., Donahue, N. M. & Pandis, S. N. (2007). Ozonolysis ~~ofupalpha~~of α-pinene at atmospherically relevant concentrations: Temperature dependence of aerosol mass fractions (yields). *J Geophys Res*, 112, doi:10.1029/2006jd007436.

Pichelstorfer, L. & Hofmann, W. (2015). Modeling aerosol dynamics of cigarette smoke in a denuder tube. *J Aerosol Sci*, 88, 72-89, doi:10.1016/j.jaerosci.2015.05.009.

1020 Pichelstorfer, L., Winkler-Heil, R., Boy, M. & Hofmann, W. (2021). Aerosol dynamics simulations of the anatomical variability of e-cigarette particle and vapor deposition in a stochastic lung. *J Aerosol Sci*, 158, 105706, doi:10.1016/j.jaerosci.2020.105706.

Pierce, J. R., Engelhart, G. J., Hildebrandt, L., Weitkamp, E. A., Pathak, R. K., Donahue, N. M., Robinson, A. L., Adams, P. J. & Pandis, S. N. (2008). Constraining Particle Evolution from Wall Losses, Coagulation, and Condensation-Evaporation in

1025 Smog-Chamber Experiments: Optimal Estimation Based on Size Distribution Measurements. *Aerosol Sci Tech*, 42, 1001-1015, doi:10.1080/02786820802389251.

Riipinen, I., Pierce, J. R., Donahue, N. M. & Pandis, S. N. (2010). Equilibration time scales of organic aerosol inside thermodenuders: Evaporation kinetics versus thermodynamics. *Atmos. Environ.*, 44, 597-607, doi:10.1016/j.atmosenv.2009.11.022.

1030 Roldin, P., Ehn, M., Kurtén, T., Olenius, T., Rissanen, M. P., Sarnela, N., Elm, J., Rantala, P., Hao, L., Hyttinen, N., Heikkinen, L., Worsnop, D. R., Pichelstorfer, L., Xavier, C., Clusius, P., Öström, E., Petäjä, T., Kulmala, M., Vehkamäki, H., Virtanen, A., Riipinen, I. & Boy, M. (2019). The role of highly oxygenated organic molecules in the Boreal aerosol-cloud-climate system. *Nat Commun*, 10, doi:10.1038/s41467-019-12338-8.

Roldin, P., Eriksson, A. C., Nordin, E. Z., Hermansson, E., Mogensen, D., Rusanen, A., Boy, M., Swietlicki, E., Svenningsson,

1035 B., Zelenyuk, A. & Pagels, J. (2014). Modelling non-equilibrium secondary organic aerosol formation and evaporation with the aerosol dynamics, gas- and particle-phase chemistry kinetic multilayer model ADCHAM. *Atmos Chem Phys*, 14, 7953-7993, doi:10.5194/acp-14-7953-2014.

Roldin, P., Swietlicki, E., Schurgers, G., Arneth, A., Lehtinen, K. E. J., Boy, M. & Kulmala, M. (2011). Development and evaluation of the aerosol dynamics and gas phase chemistry model ADCHEM. *Atmospheric chemistry and physics*, 11, 5867-

1040 5896, doi:.

Rose, C., Chaumerliac, N., Deguillaume, L., Perroux, H., Mouchel-Vallon, C., Leriche, M., Patryl, L. & Armand, P. (2018). Modeling the partitioning of organic chemical species in cloud phases with CLEPS (1.1). *Atmos Chem Phys*, 18, 2225-2242, doi:10.5194/acp-18-2225-2018.

Sandu, A., Verwer, J., Blom, J., Spee, E., Carmichael, G. & Potra, F. (1997). Benchmarking stiff ode solvers for atmospheric

1045 chemistry problems II: Rosenbrock solvers. *Atmos. Environ.*, 31, 3459-3472, doi:10.1016/s1352-2310(97)83212-8.

Saunders, S. M., Jenkin, M. E., Derwent, R. G. & Pilling, M. J. (2003). Protocol for the development of the Master Chemical Mechanism, MCM v3 (Part A): tropospheric degradation of non-aromatic volatile organic compounds. *Atmos Chem Phys*, 3, 161-180, doi:10.5194/acp-3-161-2003.

Seinfeld, J. H. & Pandis, S. N. (2016). *Atmospheric Chemistry and Physics - From Air Pollution to Climate Change*. : Wiley-

1050 Interscience.

Shiraiwa, M., Pfrang, C. & Pöschl, U. (2010). Kinetic multi-layer model of aerosol surface and bulk chemistry (KM-SUB): the influence of interfacial transport and bulk diffusion on the oxidation of oleic acid by ozone. *Atmos Chem Phys*, 10, 3673-3691, doi:10.5194/acp-10-3673-2010.

Smith, J. N., Draper, D. C., Chee, S., Dam, M., Glicker, H., Myers, D., Thomas, A. E., Lawler, M. J. & Myllys, N. (2021).

1055 Atmospheric clusters to nanoparticles: Recent progress and challenges in closing the gap in chemical composition. *J Aerosol Sci*, 153, 105733, doi:10.1016/j.jaerosci.2020.105733.

von Smoluchowski, M. (1918). Versuch einer mathematischen Theorie der Koagulationskinetik kolloider Lösungen. *Zeitschrift für Physikalische Chemie*, 92U, 129-168, doi:10.1515/zpch-1918-9209.

Su, T. & Chesnavich, W. J. (1982). Parametrization of the ion–polar molecule collision rate constant by trajectory calculations. *J. Chem. Phys.*, 76, 5183-5185, doi:10.1063/1.442828.

Topping, D., Connolly, P. & Reid, J. (2018). PyBox: An automated box-model generator for atmospheric chemistry and aerosol simulations.. *Journal of Open Source Software*, 3, 755, doi:10.21105/joss.00755.

Tsang, T. H. & Brock, J. R. (1982). Simulation of Condensation Aerosol Growth by Condensation and Evaporation. *Aerosol Sci Tech*, 2, 311-320, doi:10.1080/02786828308958637.

Valorso, R., Aumont, B., Camredon, M., Raventos-Duran, T., Mouchel-Vallon, C., Ng, N. L., Seinfeld, J. H., Lee-Taylor, J. & Madronich, S. (2011). Explicit modelling of SOA formation from upalpha-pinene photooxidation: sensitivity to vapour pressure estimation. *Atmos Chem Phys*, 11, 6895-6910, doi:10.5194/acp-11-6895-2011.

Vignati, E., Wilson, J. & Stier, P. (2004). M7: An efficient size-resolved aerosol microphysics module for large-scale aerosol transport models. *Journal of Geophysical Research: Atmospheres*, 109, n/a-n/a, doi:10.1029/2003jd004485.

Wagner, P. E. (1982). Aerosol Growth by Condensation. In (Eds.), *Topics in Current Physics* (pp. 129-178). : Springer Berlin Heidelberg.

Whitby, E. R. & McMurry, P. H. (1997). Modal Aerosol Dynamics Modeling. *Aerosol Sci Tech*, 27, 673-688, doi:10.1080/02786829708965504.

Xavier, C., Baykara, M., de Jonge, R. W., Altstädter, B., Clusius, P., Vakkari, V., Thakur, R., Beck, L., Becagli, S., Severi, M., Traversi, R., Wehner, B., Sipilä, M., Kulmala, M., Boy, M. & Roldin, P. (2022). Secondary aerosol formation in marine Arctic environments: A model measurement comparison at Ny-Å#lesund#. , , doi:10.5194/acp-2022-200.

Xavier, C., Rusanen, A., Zhou, P., Dean, C., Pichelstorfer, L., Roldin, P. & Boy, M. (2019). Aerosol mass yields of selected biogenic volatile organic compounds – a theoretical study with nearly explicit gas-phase chemistry. *Atmos Chem Phys*, 19, 13741-13758, doi:10.5194/acp-19-13741-2019.

Yli-Juuti, T., Barsanti, K., Ruiz, L. H., Kieloaho, A.-J., Makkonen, U., Petäjä, T., Ruuskanen, T., Kulmala, M. & Riipinen, I. (2013). Model for acid-base chemistry in nanoparticle growth (MABNAG). *Atmos Chem Phys*, 13, 12507-12524, doi:10.5194/acp-13-12507-2013.

Zhang, Q., Jimenez, J. L., Canagaratna, M. R., Allan, J. D., Coe, H., Ulbrich, I., Alfarra, M. R., Takami, A., Middlebrook, A. M., Sun, Y. L., Dzepina, K., Dunlea, E., Docherty, K., DeCarlo, P. F., Salcedo, D., Onasch, T., Jayne, J. T., Miyoshi, T., Shimono, A., Hatakeyama, S., Takegawa, N., Kondo, Y., Schneider, J., Drewnick, F., Borrmann, S., Weimer, S., Demerjian, K., Williams, P., Bower, K., Bahreini, R., Cottrell, L., Griffin, R. J., Rautiainen, J., Sun, J. Y., Zhang, Y. M. & Worsnop, D. R. (2007). Ubiquity and dominance of oxygenated species in organic aerosols in anthropogenically-influenced Northern Hemisphere midlatitudes. *Geophys Res Lett*, 34, n/a-n/a, doi:10.1029/2007gl029979.

Zhang, X., Cappa, C. D., Jathar, S. H., McVay, R. C., Ensberg, J. J., Kleeman, M. J. & Seinfeld, J. H. (2014). Influence of vapor wall loss in laboratory chambers on yields of secondary organic aerosol. *Proc. Natl. Acad. Sci.*, 111, 5802-5807, doi:10.1073/pnas.1404727111.

Zhang, Y., Seigneur, C., Seinfeld, J. H., Jacobson, M. Z. & Binkowski, F. S. (1999). Simulation of Aerosol Dynamics: A Comparative Review of Algorithms Used in Air Quality Models. *Aerosol Sci Tech*, 31, 487-514, doi:10.1080/027868299304039.